

Precision Herbicide Sprayer for an Agricultural Robot



Prepared by:

Kayuran Naicker
NCKKAY002

Department of Electrical Engineering
University of Cape Town

Prepared for:

Boitumelo Dikoko

Department of Electrical Engineering
University of Cape Town

October 2023


Submitted to the Department of Electrical Engineering at the University of Cape Town in partial fulfilment of the academic requirements for a Bachelor of Science degree in Mechatronics Engineering

Key Words: Agricultural, Herbicide, AI vision, Weed control

Declaration

1. I know that plagiarism is wrong. Plagiarism is to use another's work and pretend that it is one's own.
2. I have used the IEEE convention for citation and referencing. Each contribution to, and quotation in, this final year project report from the work(s) of other people, has been attributed and has been cited and referenced.
3. This final year project report is my own work.
4. I have not allowed, and will not allow, anyone to copy my work with the intention of passing it off as their own work or part thereof
5. Word count of body: 15684 words.

Name: Kayuran Naicker

Signature: 

Date: 30 October 2023

Terms of Reference

This final year project is focused on the development of a herbicide application system. This system entails the design, fabrication, and evaluation of a set of nozzles capable of accurately dispensing herbicide onto targeted weeds. This system should be able to autonomously identify and select weed targets for herbicide application.

The final design must include a base to house all the required components and be capable of traversing smoothly over level surfaces. Additionally, a form of target identification should be integrated into the system to enable the system to run with minimal human interaction.

Acknowledgements

I would like to express my gratitude to my supervisor, Boitumelo Dikoko, for his guidance and support throughout my research project. His approachability and encouragement made our meetings truly enjoyable and productive.

A special thanks goes out to the dedicated technical staff at UCT, namely Brendon, Riyaad, and Uzair, who offered guidance and assistance with the physical build of my prototype.

In addition, I want to express my deep gratitude to my parents, Govan and Roshni, for their financial support and for always believing in my dreams. Their constant motivation has been the driving force behind my journey. My sister, Pravania, has been an incredible pillar of strength and support throughout my university journey, always there to listen to my problems and put a smile on my face. Their presence in my life is a source of strength and inspiration.

In addition, I want to extend my appreciation to my girlfriend, Sanjana, and our friends, who provided motivation during the ups and downs of this journey, making even the most challenging moments more bearable.

Abstract

In response to the increasing demands of global food production driven by population growth, a shift from traditional farming methods towards automation has become necessary. Manual application of herbicides and chemicals in farming practices has led to an excess of chemicals in the environment, potentially endangering the health of workers and causing environmental contamination [1, 2]. To mitigate these risks, precise chemical application methods are crucial, this ensures harmful chemicals are only used where essential and thus reduces the amount of chemicals used.

In this paper, an autonomous precision herbicide robot is developed and tested. The robot autonomously locates and targets specific weeds within a designated test area of 120cm*40cm. This paper provides an overview of the current state of the art regarding agricultural robotics, thereafter, proceeding into the detailed design and testing of the robotic system. The system comprises three tightly integrated systems: nozzle actuation, liquid dispensing, and overall robot mobility. A comprehensive evaluation and testing process of multiple designs are conducted to make a well-informed decision regarding the final robot design, this includes the physical method of nozzle actuation along with tests evaluating the optimal nozzle designs and mounting height.

The study concludes that the system effectively and accurately targets weeds within the specified region. However, it is noted there are dead zones produced, due to the configuration of the robot, where weeds cannot be targeted. Recommendations to address this issue are presented.

Table of Contents

Declaration	i
Terms of Reference.....	ii
Acknowledgements	iii
List of Figures	viii
1. Introduction.....	1
1.1 Background to the study	1
1.2 Objectives of this study	1
1.2.1 Problems to be investigated.....	1
1.2.2 Purpose of the study	1
1.3 Scope and Limitations	1
1.4 Plan of development	1
2. Literature Review	2
2.1 Navigation and Mobility.....	3
2.2 Object Detection and Targeting Weeds.....	4
2.2.1 Basic Differentiation of Elements on the Test Ground.....	4
2.2.2 Establishing a Target	5
2.2.3 Motion Control and Configuration of Nozzles.....	5
2.3 Dispensing of Herbicide	7
2.4 Observations	8
3. Methodology	9
3.1 Nozzle Actuation	10
3.1.1 Design One	10
3.1.2 Design Two	11
3.1.3 Design Three.....	11
3.2 Liquid Dispensing	12
3.2.1 Control and Management of the Flow of Liquid	12
3.2.2 Nozzle Design.....	14
3.3 Camera Vision	15
3.4 Cart Design	15
3.4.1 Positioning of Actuation Arms	15
3.4.2 Camera Movement	16
3.4.3 Linear Movement of Cart	17
3.5 Code Structure	18

3.5.1	Obtaining Camera Data	18
3.5.2	Allocation of Targets	19
3.5.3	Arm Actuation Algorithm	19
3.5.4	Nozzle activation	22
3.5.5	Full Control Algorithm	22
3.6	Final Circuitry	23
3.7	Final Designed Parts	24
4.	Results.....	26
4.1	Nozzle Actuation	26
4.1.1	Nozzle Angle Test	26
4.2	Arm Positioning.....	27
4.3	Nozzle Height and Design Test	29
4.4	Herbicide Volume test	31
4.5	Nozzle Accuracy Test.....	32
4.5.1	Rotational Accuracy Test	32
4.5.2	Linear Accuracy Test.....	32
4.5.3	Combined Test (single target)	33
4.5.4	Combined Test (multiple targets)	33
4.6	Camera Vision	33
4.6.1	Object Detection	33
4.6.2	Colour Detection.....	34
5.	Discussion	35
5.1	Nozzle Actuation	35
5.2	Arm Positioning.....	35
5.3	Nozzle Height and Design Test	36
5.4	Herbicide Volume Test.....	36
5.5	Nozzle Accuracy Test.....	37
5.5.1	Rotational Accuracy Test	37
5.5.2	Linear Accuracy Test.....	37
5.5.3	Combined Tests (single and multiple targets)	37
5.6	Camera Vision	38
5.6.1	Object Detection	38
5.6.2	Colour Detection.....	38
5.7	Cart Design	38
6.	Conclusions.....	39

6.1	Nozzle Actuation	39
6.2	Arm Positioning.....	39
6.3	Nozzle Height and Design Test	39
6.4	Herbicide Volume Test.....	39
6.5	Nozzle Accuracy Test.....	40
6.5.1	Rotational Accuracy Test	40
6.5.2	Linear Accuracy Test.....	40
6.5.3	Combined Test (single and multiple targets).....	40
6.6	Camera Vision	40
6.6.1	Object detection	40
6.6.2	Colour detection	40
6.7	Cart Design	40
7.	Recommendations.....	42
7.1	Dead Zone Mitigation.....	42
7.2	Revision of the Coding Structure	42
7.3	Addition of Pressure Regulator	42
7.4	Revision of Leg Design	42
8.	List of References.....	43
9.	Appendix A.....	45
10.	Appendix B.....	46
11.	EBE Faculty: Assessment of Ethics in Research Projects.....	47

List of Figures

Figure 1: Flow diagram showing the method generally used in precision herbicide robots.	2
Figure 2: A sample of robot platforms developed for different applications. (a) the Asterix robot (sourced from [2]), (b) ANYmal, a legged robot to navigate difficult terrain (sourced from [5]), and (c) a three-wheeled design for navigation of crop rows (sourced from [3]).	3
Figure 3: Image showing the locating of the stem of a crop (a) Source image (b) Image showing the computer vision algorithm estimating the stem of a plant using the centroid method, sourced from [8].	5
Figure 4: Input image from computer vision denoting a crop in red, weeds in green and background in black, sourced from [7]	6
Figure 5: A representation of the generated weed map used to control the solenoid sprayer valves. 0 denotes areas where the valve should be closed (over crops and background) and a 1 denotes where the valve should be turned on (over weeds), sourced from [7].	6
Figure 6: (a) A target weed after the DoD application of herbicide. The yellow paper emphasises the drops of herbicide that did not hit the leaf. There is no visible liquid on the leaves as satellite drops formed mid-air and bounced off the leaf. Image source sourced from [2]. (b) An image showing the different parts of a droplet ejected from a solenoid and the formation of satellite drops, sourced from [3]	7
Figure 7: (a) Results from the addition of only surfactant to the herbicide. (b) shows the results of the addition of a polymer surfactant mixture to the herbicide, sourced from [17].	8
Figure 8: Image showing a simplified model of design one.	10
Figure 9: Image showing a simplified model of design two.	11
Figure 10: Image showing a simplified model of design three.	11
Figure 11: KiCad Schematic of the Solenoid Control Circuit	12
Figure 12: 3D printed pipe connectors used to divert the flow of liquid through the system.	13
Figure 13: Image showing the different nozzle keyway designs.	14
Figure 14: Image showing a collection of 3D modelled parts in SolidWorks of the camera module system.	16
Figure 15: Full assembly of the sliding camera module, including the Huskylens camera.	16
Figure 16: KiCad wiring schematic of the push buttons utilised in the camera movement system.	17
Figure 17: Designed leg of the robot, with mounting holes to hold the wheels in place.	17
Figure 18: Coding structure to create a target map of the target region.	18
Figure 19: MATLAB simulation showing the allocation of targets, specified by coloured blocks to represent which arm a specific target would get allocated to.	19
Figure 20: Image showing the different regions a coordinate could fall under relative to the actuation arm pivot point, indicated by the red dot.	20
Figure 21: Diagram showing the positioning of a coordinate in region one.	20
Figure 22: Coding structure to convert 'World Coordinate array' to array of rotational and linear actuation.	21
Figure 23: Image showing the code used to activate the pump and solenoid when required.	22
Figure 24: Image showing a simplified structure of the full control algorithm code.	22
Figure 25: Image showing the wiring schematic of the Arduino board.	23
Figure 26: Image showing all parts for the arm actuation system, modelled in SolidWorks.	24
Figure 27: Full assembly of the actuation arm fitted with the stepper motors and mounted onto the prototype.	25
Figure 28: Image showing the full assembly of the precision herbicide sprayer prototype. (A) Microcontroller, (B) Actuation Arm, (C) Camera Movement System, (D) Liquid Dispensing pump and (E) Motorized Wheel.	25
Figure 29: MATLAB simulations of reachable target locations of Design Two (a) and Design Three (b).	26
Figure 30: Image showing the change in the pattern of the deposited liquid with a change in the angle of the nozzle. (a) shows the nozzle mounted at the central position of 0°, (b) at 15°, (c) at 30°, (d) at 45° and lastly (e) at 60° from the central position.	26
Figure 31: MATLAB simulations showing a mapping of reachable target locations of Design 3, utilising various arm lengths positioned at pivot point one, which is along the edge of the target region. Plots are labelled above the respective plots.	27

Figure 32: MATLAB simulations showing a mapping of reachable target locations of Design 3, utilising various arm lengths positioned at pivot point two, which is along the central line of the target region. Plots are clearly labelled above the respective plot.....	28
Figure 33: Spraying pattern of a 1mm diameter keyway in the nozzle. (a) Nozzle mounted 15cm from the surface with an average splash diameter of 1.7cm, (b) Nozzle mounted 25cm from the surface with an average splash diameter of 2.6cm, (c) Nozzle mounted 45cm from the surface with an average splash diameter of 3.4cm.....	29
Figure 34: Spraying pattern of a 1.5mm diameter keyway in the nozzle. (a) Nozzle mounted 15cm from the surface with an average splash diameter of 3.5cm, (b) Nozzle mounted 25cm from the surface with an average splash diameter of 4.4cm, (c) Nozzle mounted 45cm from the surface with an average splash diameter of 5.5cm.....	29
Figure 35: Spraying pattern of a 2mm diameter keyway in the nozzle. (a) Nozzle mounted 15cm from the surface with an average splash diameter of 4.5cm, (b) Nozzle mounted 25cm from the surface with an average splash diameter of 5.5cm, (c) Nozzle mounted 45cm from the surface with an average splash diameter of 6.6cm.....	29
Figure 36: Spraying pattern of a 2.5mm diameter keyway in the nozzle. (a) Nozzle mounted 15cm from the surface with an average splash diameter of 5.6cm, (b) Nozzle mounted 25cm from the surface with an average splash diameter of 6.5cm, (c) Nozzle mounted 45cm from the surface with an average splash diameter of 7.4cm.....	29
Figure 37: Spraying pattern of a rectangular keyway in the nozzle (2.4mm*0.4mm). (a) Nozzle mounted 15cm from the surface with an average splash diameter of 1.4cm, (b) Nozzle mounted 25cm from the surface with an average splash diameter of 1.7cm, (c) Nozzle mounted 45cm from the surface with an average splash diameter of 2.5cm.	30
Figure 38: Spraying pattern of a rectangular keyway in the nozzle (2.4mm*0.8mm). (a) Nozzle mounted 15cm from the surface with an average splash diameter of 3.5cm, (b) Nozzle mounted 25cm from the surface with an average splash diameter of 4.6cm, (c) Nozzle mounted 45cm from the surface with an average splash diameter of 5.4cm.	30
Figure 39: Spraying pattern of '+' keyway in the nozzle. (a) Nozzle mounted 15cm from the surface with an average splash diameter of 2.6cm, (b) Nozzle mounted 25cm from the surface with an average splash diameter of 3.7cm, (c) Nozzle mounted 45cm from the surface with an average splash diameter of 4.6cm.	30
Figure 40: Images showing the accuracy of the system when targeting a single point.	33
Figure 41: Images from the Huskylens object detection setting identifying the difference between crops and weeds; (a) correct identification of a crop, (b) correct identification of a weed, (c) inaccurate identification of objects given that there are two objects in one frame, (d) incorrect identification of an object.	34
Figure 42: Images utilising the Huskylens colour detection function identifying coloured stickers with the camera mounted at different heights, (a) camera mounted at a height of 25cm from the surface, (b) camera mounted at 45cm from the surface, (c) camera mounted at 65 cm from the surface.....	34

List of Tables

Table 1: Table summarizing the functional requirements of the prototype. 9

Table 2: Table summarizing the acceptance criteria for the prototype. 9

Table 3: Descriptions of functions defined in the control algorithm code. 23

Table 4: Showing the change in the average width of the deposited liquid relative to the change in nozzle angle. 27

Table 5: Showing the effect of mounting height of different nozzles and the average diameter of the deposited liquid.
..... 31

Table 6: Showing the average volume of liquid deposited from each solenoid. 31

Table 7: Showing the results of the accuracy test on the rotational arm actuation. 32

Table 8: Showing the results of the accuracy test on the rotational arm actuation. 32

1. Introduction

1.1 Background to the study

Due to the growing population, the need for food security becomes evident, thus automation of traditional farming methods is necessary. The yield of a crop is greatly dependant on the control of weeds in a field [2], weeds compete with the crop for essential resources such as sunlight and nutrients in the soil. Manual application of herbicides and chemicals in farming practices has led to an excess amount of chemicals released into the environment causing environmental contamination. In addition to this, the application process poses health risks to workers as these chemicals could enter the workers' bodies through their respiratory system [1]. The automation process of herbicide application would offer advantages to both workers, by reducing their exposure and ensuring minimal environmental impact during farming operations.

1.2 Objectives of this study

1.2.1 Problems to be investigated

The study's objectives encompass the development of an autonomous herbicide dispensing robot, focusing on achieving the highest precision in liquid dispensing. Additionally, a brief exploration of AI-driven target identification will be conducted.

1.2.2 Purpose of the study

Development of this robot would result in a smaller quantity of chemicals used in the application process of herbicides, thus reducing the negative effects of an excess amount of these harmful chemicals in the environment. Furthermore, the implementation of this prototype holds the potential to significantly enhance operational efficiency on farms. With the introduction of automated systems, the herbicide application process can be accelerated, farmers can treat larger fields with higher efficacy and in a more time-effective manner.

1.3 Scope and Limitations

The scope of this project encompasses the design and development of an automated precision herbicide sprayer. This involves building the robotic system from the ground up, including the body of the robot, as well as designing and modelling all the necessary components. The integration of an AI-powered camera serves as an element for target identification, enabling autonomous functionality. Testing of various nozzle designs is conducted in this investigation, and the relevant findings are recorded. The AI camera is trained in colour detection to maximize its capabilities.

Given the time constraint, complete integration of the AI camera into the final prototype is pending. The presented prototype processes the ability to take in an array of random coordinates and perform the precise dispensing of liquid at these designated positions.

1.4 Plan of development

This project report starts with a comprehensive literature review, where the current state of the art of agricultural robots is deeply researched, thereafter the proposed system for this prototype is introduced in the Methodology section. This methodology section is structured in chronological order of the development of the robot, drawing on conclusions of subsequent sections to continue the development process. The uniform use of headings across the Results, Discussion, and Conclusion sections provides a clear and organized structure for presenting and analysing the project's findings. This structure enhances the reader's ability to follow and grasp the information presented in each section.

2. Literature Review

As the demand for food production rises and the necessity for sustainable farming practices becomes more evident, there is a growing movement towards the automation of farming methods, thus there is a large body of research ongoing. This chapter reviews the current state of the art of agricultural robots, and the relevant literature is critiqued and summarized. Gaps in the current literature are located and areas of further research are identified.

Figure 1 shows a generalized structure utilised by agricultural robots. Firstly, objects on the field need to be identified into their respective categories, which would be differentiating between the soil, plants, pests, fruit, and weeds. Thereafter this information is used to produce a target map; where the spraying algorithm plays a pivotal role in determining which nozzles will be utilised. Robotic arm actuation is used to direct high-precision nozzles at the desired location. Thereafter the relevant amount of herbicide can be dispensed. This literature review is presented starting with (1)Navigation and Mobility moving onto (2)Object Detection and Targeting weeds finally ending with the (3)Dispensing of Herbicides and (4)Observations.

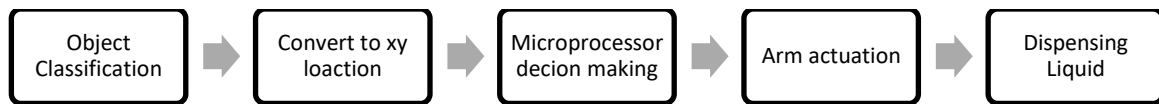


Figure 1: Flow diagram showing the method generally used in precision herbicide robots.

2.1 Navigation and Mobility

Navigation across the terrain is an essential initial milestone for the robot, facilitating its seamless interaction with the surrounding environment. There have been numerous diverse designs of agricultural robots, presented by various companies with unique features tailored to achieve precise navigation within specific environments and cater to distinct operational requirements. This section provides a very brief overview of the navigation strategies used in agricultural robots.

To navigate crop fields a robust and compact design is required (fields often consist of rows of vegetation very close to one another)[3]. Robots making use of a three-wheeled design is an uncommon practice in the field of farming, although this approach was utilised in an asymmetric configuration to make it more conducive to the navigation of rows without damaging the crop [2], this is shown in Figure 2(c). This enabled a lighter design with only two motorized axes and a fixed wheel suspension.

An alternative approach to land vehicles for the distribution of herbicides would be through the use of drones. However, it should be noted that this method was shown to work better in cases where a more even spread of a chemical is required over a large area [4], and not very cost-effective for localized applications as needed in our case. The following images showcase a compilation of robots created by various individuals, encompassing those employed in agriculture as well as others that highlight the diverse navigational capabilities of robotic systems.

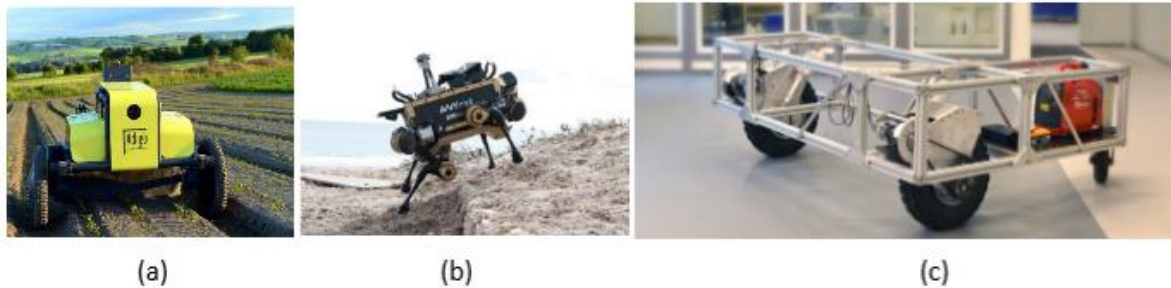


Figure 2: A sample of robot platforms developed for different applications. (a) the Asterix robot (sourced from [2]), (b) ANYmal, a legged robot to navigate difficult terrain (sourced from [5]), and (c) a three-wheeled design for navigation of crop rows (sourced from [3]).

The above-mentioned designs pose as a very brief overview of the field of agricultural robots and do not pose as a complete overview of the state of the art, numerous other systems implement the similar task.

After achieving a degree of mobility, the next objective of agricultural robots is the task of object detection capabilities.

2.2 Object Detection and Targeting Weeds

The ability to detect and classify the surroundings is essential to the functioning of agricultural robots. There needs to be a clear differentiation between the background, crop, and weeds. Due to the rapid growth in machine learning and sophisticated algorithms, there has been great development in the field of crop-weed classification. Various methods have been investigated from comparing leaf contours [6] to using coloured dyes on young seedlings to differentiate from weeds[7]. Object detection is not only limited to differentiating between the various elements in the field but also entails a means of determining a strategic target location for the application of herbicide. It is often required to identify the stem/centroid of the plant to optimize herbicide application targeted at the stem of the weed as explored in [8, 9].

2.2.1 Basic Differentiation of Elements on the Test Ground

It was presented in [6], that a common plant recognition method used in the industry utilises colour segmentation as one of the first steps to distinguish plants from the soil. This method could be used in situations where weeds and the crop have a distinct colour differentiation. To utilise this idea of distinct colour differentiation between not only the soil and plants but also crops and weeds (where they are both green), a test where the desired crops were treated with a water-based latex paint before transplanting outdoors[7]. This method produced favourable results, although it can only be utilised where the crops are established seedlings free of weeds, this method does not provide a solution during the early development stages of the seedling.

Many of the vision-based technologies rely on clear imagery for processing. Under ideal conditions, these methods would have a higher success rate but given that these robots are deployed into the natural environment there is a significant amount of uncertainty involved. The sun exposure on the captured images significantly impacts the computational performance of the algorithms utilised. Another important factor to take into consideration is that the plant leaves should remain undamaged and free of visible signs of stress to be accurately identified as the correct type of crop or weed [6]. To ensure the clarity of the images and mitigate the effect of wind disturbance in the system, the test area could be enclosed with a tractor-mounted hood with controlled illumination when analysing the test group of plants as done in [10]. This would result in a more controlled environment to increase the success rate of the deployed object detection algorithm.

2.2.2 Establishing a Target

To determine a specific target location for the application of herbicide, an analysis of the plant structure is taken into consideration. The stem of the weed is targeted for the application of herbicide as it supports the entire plant, this would effectively kill a weed with the correct application of herbicide. The stem position was defined to be at the centroid of the vegetation in [8], this implementation can be seen in Figure 3, This approach yielded suboptimal results, as its implementation proved ineffective in scenarios where weeds lack symmetry or overlap with one another.

Another method of stem detection explored in the paper [11], makes use of the contours of individually detected leaves, this method did not produce favourable results, again due to the overlapping of leaves and irregular shapes of leaves. Furthermore, the algorithm that was employed generated a significant number of false positives, further distorting the data set. Thus, a more precise method of stem detection is required. To ensure clear images are captured for processing, LEDs can be used to properly illuminate the imaging region as done in the work [7].

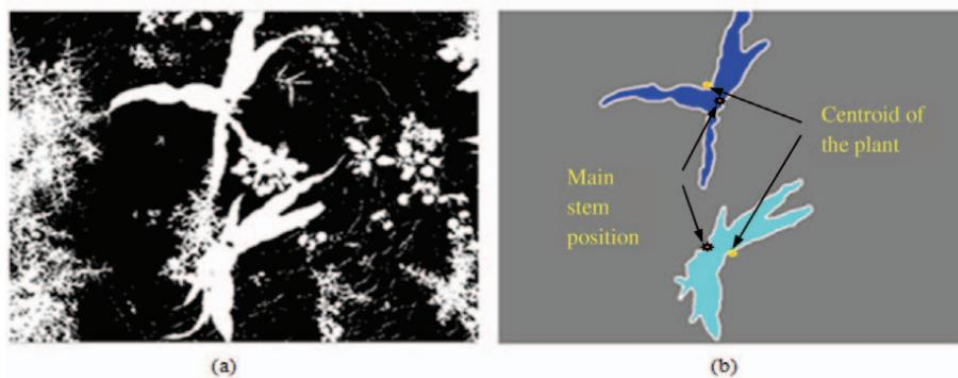


Figure 3: Image showing the locating of the stem of a crop (a) Source image (b) Image showing the computer vision algorithm estimating the stem of a plant using the centroid method, sourced from [8].

2.2.3 Motion Control and Configuration of Nozzles

Defining the optimal way to control the motion and spraying algorithm of the robot would greatly affect the efficiency of its ability to cover a larger area. How the robot analyses its surroundings is essential to path determination and overall operational efficiency.

In the paper by T. Meshram et al. [1], an approach that stops the robot at each crop to detect pests and then continues its path was utilised. Even though this method did prove itself to be successful the continuous stopping of the robot costs valuable time and would increase the time required to cover a larger field.

K. Jensen et al. utilised hydraulic nozzles adapting a continuous application method to decrease the time required to start and stop the valves [12]. The hydraulic valve was activated before reaching the target location to ensure the nozzle produced its full output at the desired location, thereafter the nozzle was manoeuvred over other target locations and only closed after the final location was reached. This method is not very efficient since the valves are constantly open, releasing herbicide on the soil rather than strategically on the weeds.

To determine a more precise method of herbicide application a 12-sprayer design utilised by R. Raja et al. [7], made use of a weed-treating map to determine the locations of weeds and program how long each nozzle should be on for. The 12 nozzles were positioned in an array that provided a 120mm wide sprayer with individual sprayer modules covering a 10mm band. This formation of nozzles allowed the weed-treating map to be generated using pixel-based mapping. This method requires an image denoting the crop, weed, and background in separate colours (Figure 4), thereafter a grid was applied over the image and either filled in with a 1 or 0, depending on if there is a weed in that pixel, this can be seen in Figure 5. Each row on Figure 5 indicates the position of one of the sprayer heads, thus as the sprayer moves from left to right, if a cell is denoted with a 1 the valve would turn on and remain on until the pixel at that position corresponds to 0. This enables accurate targeting of weeds.



Figure 4: Input image from computer vision denoting a crop in red, weeds in green and background in black, sourced from [7]

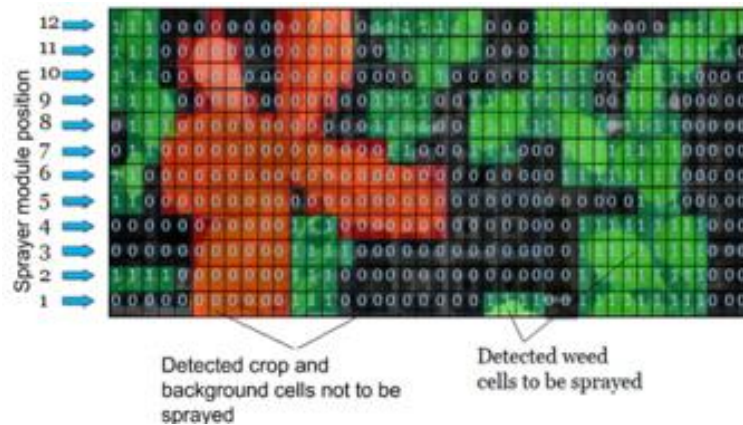


Figure 5: A representation of the generated weed map used to control the solenoid sprayer valves. 0 denotes areas where the valve should be closed (over crops and background) and a 1 denotes where the valve should be turned on (over weeds), sourced from [7]

It was noted in the results of [7] that due to the proximity of some of the weeds to the crop, the algorithm could not target these weeds as the priority was to save the crop. The design decision to place the array of nozzles behind the camera allowed for enough computational time before action is required.

After establishing the exact target location for the herbicide application, the focus shifts to optimizing the dispensing process. In the next section, we explore strategies for precise and efficient herbicide application.

2.3 Dispensing of Herbicide

The development of an accurate and precise dispensing structure is essential to minimize the effect of toxic chemicals released into the environment [1] and to protect the desired crops. The dispensing of liquid is broadly divided into two categories, either utilising a drop-on-demand method or a jet sprayer method. Both methods have their limitations and pros, which are investigated below.

The Asterix robot [2], utilises a drop-on-demand (DoD) method of dispensing herbicide, making use of an extensive 28 nozzles for the herbicide application. This DoD method targets the leaves of the weed, it was observed that satellite drops (small drops lagging the main droplet) formed mid-air and had poor herbicide retention on the leaves. This can be seen in Figure 6(a). The fluid dynamics of these droplets were thoroughly investigated in the paper [3]. It is noted that upon ejection of the droplet from the valve, the droplet consisted of 3 main sections, this can be seen in Figure 6(b), thereafter the droplet can undergo several scenarios. The filament may be absorbed into the main droplet, the filament may break away from the main droplet creating a single satellite drop or instability may occur in the droplet and create multiple satellite droplets behind the main droplet [13].

It was presented in [14], that under ideal conditions the satellite droplets will catch up with the main drop and strike the target as a single droplet, given that the falling distance is long enough, this distance would differ with different liquids. Since this model will be deployed in a natural environment there will likely be atmospheric disturbances such as wind that will hinder the accuracy of the DoD method. The filament stability is determined by the viscosity, density and surface tension of the liquid used [15], thus a deep analysis of every different herbicide utilised would be required to accurately calibrate the system to ensure accuracy. This uncertainty associated with the satellite drops adds a layer of complexity to the testing process of the DoD method. This process requires a very close examination of the drops and a deep understanding of fluid dynamics.

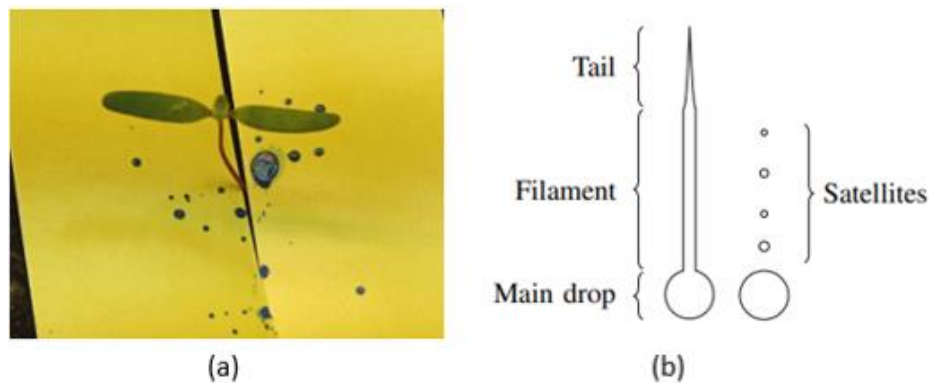


Figure 6: (a) A target weed after the DoD application of herbicide. The yellow paper emphasises the drops of herbicide that did not hit the leaf. There is no visible liquid on the leaves as satellite drops formed mid-air and bounced off the leaf. Image source sourced from [2]. **(b)** An image showing the different parts of a droplet ejected from a solenoid and the formation of satellite drops, sourced from [3]

Another common method for applying herbicide onto weeds involves the use of jet sprayer nozzles. To ensure proper operation of jet spray nozzles, it was noted in [16] that the total flow rate per nozzle must be maintained at a constant value. If the flow rate is too high the produced droplet size will be too small, making the produced spray more susceptible to drift, if too low the covered surface area is reduced. This method utilises individual nozzles each covering a large surface area, thus the pressure must be carefully maintained.

The approach using jet spray nozzles was utilised by R. Raja et al. [7], 12 sprayer modules comprising of a solenoid and plunger assembly were mounted onto a body, this configuration was necessary for the specific spraying algorithm used in this machine as mentioned in the ‘Motion control and configuration of nozzles’ section. It was noted in the research by R. Raja et al. that the optimal valve operating conditions were determined by trial-and-error. Scaling this design for larger applications proves to be expensive, requiring nozzles placed every 10 mm, thereby escalating costs significantly. Beyond financial concerns, maintaining numerous nozzles poses logistical challenges, with clogs in even one nozzle disrupting the treatment of an entire weed row. This system is not very robust.

To mitigate splashing upon impact of a microjet spray, the inherent properties of the liquid utilised must be investigated. In the study conducted by Downey et al. [17], an evaluation of both the effects of the splashing and the coverage area of the micro jet sprayer was reported. It was noted in their research that the addition of surfactants decreases the surface tension of a liquid but increases the surface deposition of the liquid, and polymers reduce the splashing of the liquid upon impact. The results from this test can be seen in Figure 7. Due to the addition of the surfactant, there is a significant splash present in (a), this issue is resolved with the addition of polymers in (b). This methodology provides a possible solution to mitigate the effects of stray splashing from the jet sprayers.

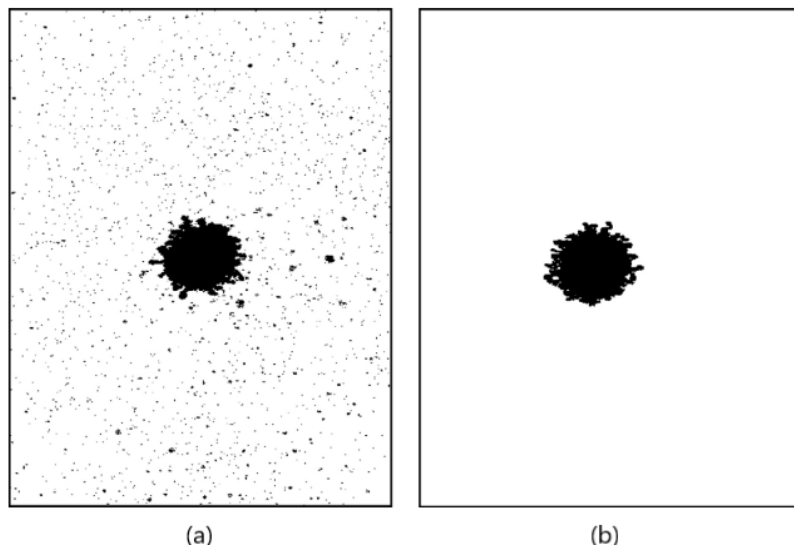


Figure 7: (a) Results from the addition of only surfactant to the herbicide. (b) shows the results of the addition of a polymer surfactant mixture to the herbicide, sourced from [17].

It was documented in [2], that most herbicides are corrosive liquids and if they are left in the valve system, they will leave behind a residue. These residues can hinder the ability of the valves from sealing correctly thus resulting in leaking valves that could damage other crops. It concluded that the system should be flushed regularly with clean water to avoid the build-up of unwanted residue and the valves should be thoroughly cleaned when left unused for an extended period.

2.4 Observations

The above literature review covers the foundational methods presently employed and under experimental investigation within the field of agricultural robots. It was noted that the trend in precision herbicide sprayers previously developed has been inclined toward either uniform herbicide dispersion using jet sprays or the adoption of Drop-on-Demand (DoD) methodologies.

There isn't a significant body of research around the use of jet nozzle sprayers utilised for precision farming. Furthermore, another gap located in this field of research was the necessity of addressing these challenges while on a strict budget, most systems comprise of multiple nozzles and highly advanced testing methodologies.

3. Methodology

After gaining a comprehensive understanding of the current state of the art pertaining to the development of agricultural robots, informed design decisions can be made to develop the prototype robot for this project.

Given the intricate nature of this system, consisting of numerous systems closely integrated, it was decided to break the system up into smaller subsystems. Each of these subsystems are further detailed below regarding chosen components, design iterations and potential tests to determine the accuracy of each subsystem. The main subsystems of this robot include Nozzle Actuation, Liquid Dispensing, Camera Vision and Cart Design. Thereafter the coding structure and final circuit are defined.

This prototype will be developed on the Arduino platform due to its user-friendly interface. The chosen board is the Arduino Mega 2560 as it has a fair amount of general-purpose input/output (GPIO) pins, that would be required to interface the entire system.

A set of function requirements and acceptance criteria were formulated to assess the performance of the system. The functional requirements of the designed prototype are outlined in Table 1 below, and the acceptance criterion in Table 2.

Table 1: Table summarizing the functional requirements of the prototype.

Requirement ID	Description of requirement
RQ-01	The system must be able to target any coordinate within the target region of 120cm*40cm.
RQ-02	The system must demonstrate precise dispensing of herbicide at the designated target location
RQ-03	The system must be able to differentiate between two distinct types of data from the test region (crop and weed target) and provide the location of the targets.

Table 2: Table summarizing the acceptance criteria for the prototype.

Requirement ID	Acceptance Criteria
RQ-01	The system must be able to acuate a nozzle to any coordinate in the specified test region.
RQ-02	The centre of the liquid deposited must be on the target location with a maximum allowable deviation of 0.5cm from the target location in any direction.
RQ-03	The system must be able to generate two arrays of coordinates, one containing the locations of the crops and the other containing the location of the weeds.

3.1 Nozzle Actuation

The placement and method of actuation for the nozzles play an important role in shaping the final design of the prototype robot. This section will introduce three distinct designs, followed by a comprehensive analysis that includes an overview of the testing done to determine the optimal design for this prototype. Conclusions for this section were used to continue the prototyping process presented in further subsections.

This section aims at addressing the functional requirement RQ-01, pertaining to the ability of the prototype to target a location in the specified target region.

3.1.1 Design One

This design entails producing an array of nozzles which will have two degrees of freedom (DOF). These nozzles will be capable of directional adjustment along both their x and y axes while remaining stationary at the central pivot point. This configuration is illustrated in Figure 8, with the x and y axis represented by the red and blue lines respectively. The maximum angle the nozzle would have to move in either the x or y axis is 60° if the nozzle is mounted at a height of 15cm from the surface. These figures were simply calculated for the explanation of the design. Effectively, this design enables the directed emission of liquid in various directions from a fixed point, targeting points while the pivot point of the nozzle remains stationary.

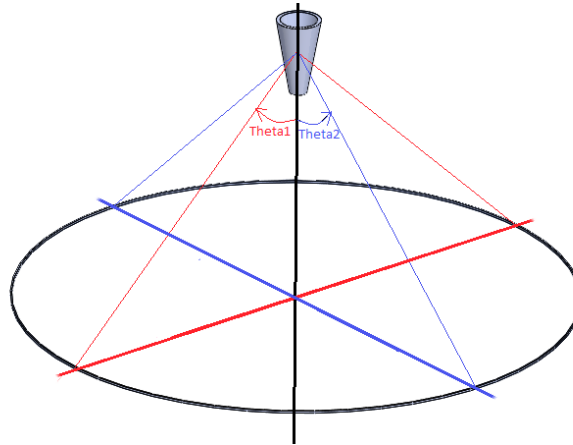


Figure 8: Image showing a simplified model of design one.

However, it is crucial to consider the impact of actuating the nozzle at an angle on the resultant spray pattern produced at ground level. To determine the effect of this, the 1mm diameter nozzle was used to determine the change in the deposited liquid pattern on the surface, since we are simply testing the effect of the nozzle angle the size of the nozzle keyway does not play an important role in this test.

It is assumed that due to the effects of gravity, having the nozzle mounted at an angle would not only affect the pattern of the deposited liquid but also allow satellite drops [14] to cause splashing on sites other than the intended target area, that is between the pivot point of the nozzle and the targeted site.

3.1.2 Design Two

This design utilises a two-arm configuration with two degrees of freedom (2 DOF), the two links are driven by independent motors. Positioned at each pivot point, a stepper motor will regulate the motion of the respective arm. Each link will be able to move in an arc illustrated in Figure 9.

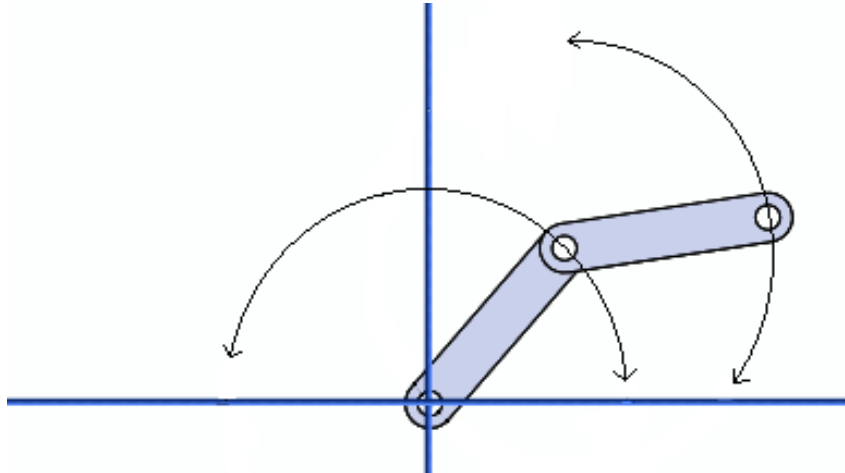


Figure 9: Image showing a simplified model of design two.

In order to evaluate this design's efficiency, the reachable arm locations will be simulated using MATLAB, these outcomes will be presented in the Results section. This analysis provides an insight into the design's capabilities and limitations, allowing for a well-informed decision to be reached.

3.1.3 Design Three

This design integrates two distinct motion components utilising a single actuation arm, utilising both rotational and linear elements. This approach involves the rotation of an arm around a central pivot point with adjustable length to precisely target specific regions within the desired range. Arcs of movement are illustrated in Figure 10.

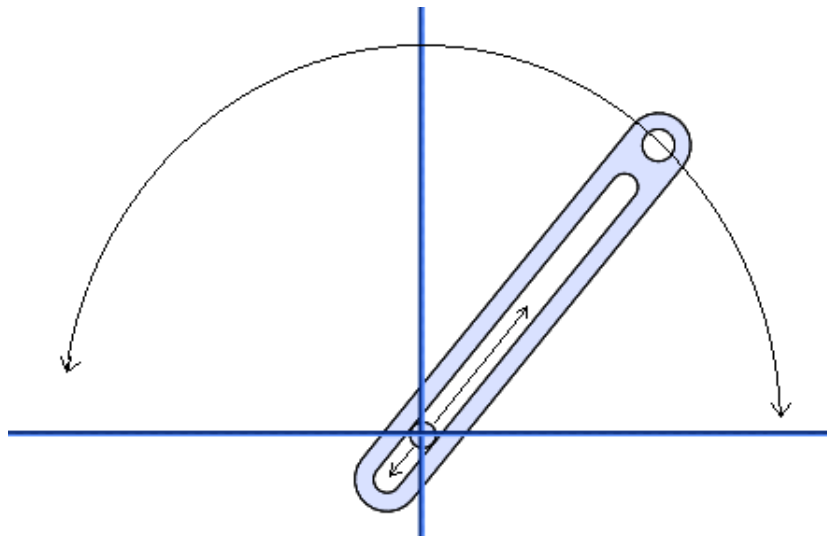


Figure 10: Image showing a simplified model of design three.

This design will make use of a rack and pinion system to achieve the extension of the arm. A housing unit would have to be designed to hold the rack and gear system in place to translate the linear motion. This entire assembly, including the rack and pinion system, will be attached to another stepper motor, which will be responsible for the rotational movement of the housing and arm.

3.2 Liquid Dispensing

Within the topic of liquid dispensing, it is important to address two primary sections. The first pertains to the regulation and flow of liquid throughout the system, and the second aspect involves the design and testing of the nozzles themselves. The dispersion pattern of the deposited liquid to achieve the highest level of accuracy is investigated to fulfil function requirement RQ-02. The integration of these two sections will be used to achieve the desired outcome of the prototype.

3.2.1 Control and Management of the Flow of Liquid

The herbicide should be contained within a central distribution tank from which herbicide can be sourced and transported to each nozzle. This process will be facilitated through the use of a central water pump and strategically placed solenoid valves, derived from the system presented in the works [3, 7].

The chosen water pump has a pressure rating of 100KPa (1 Bar) which will provide ample pressure to form a strong jet of liquid ejected from the nozzles. This pressure level also accounts for potential losses in the piping system, stemming from the connectors utilised. This pump requires a 12V DC supply and has an estimated flow rate greater than 220ml per 10 seconds. Verification of this flow rate will be conducted through a testing procedure documented in the results section. The actual flow rate at the output of the nozzles will not necessarily be the same as stated on the pump's data sheet since the liquid would have to go through multiple control systems before being deposited from the nozzle. Determining the precise flow rate is vital as it forms the basis of accurately determining the dosage of herbicide to be applied to a specific weed. This would ensure the herbicide application is effective and can be tailored to the specific requirements of each weed, thus optimizing the efficiency of the process.

Solenoid valves are used to control the flow of liquid/air through a system. The chosen solenoid valve for this prototype has a rated value of 12V and operates at a minimum pressure of 3Psi which is roughly 0.2 Bar, thus the chosen water pump provides enough pressure to operate this valve. The valve functions in a normally closed state, meaning that it requires a signal to open the valve, otherwise, it will remain closed under all other circumstances. To produce the 12V signal required to operate the valve, a simple control circuit is implemented to interface the solenoid with the Arduino. A TIP122 transistor is utilised as the switching component of this circuit along with a 1N4004 Diode and a 1K resistor, these components are wired together as shown in Figure 11. This circuit utilises a low-voltage signal from an Arduino GPIO pin as a trigger to connect the common ground (GND) line to the solenoid valve thereby completing its circuitry and turning on the solenoid for a specific duration. It is easier to manage the switching with the GND line due to the lower current flowing through this line.

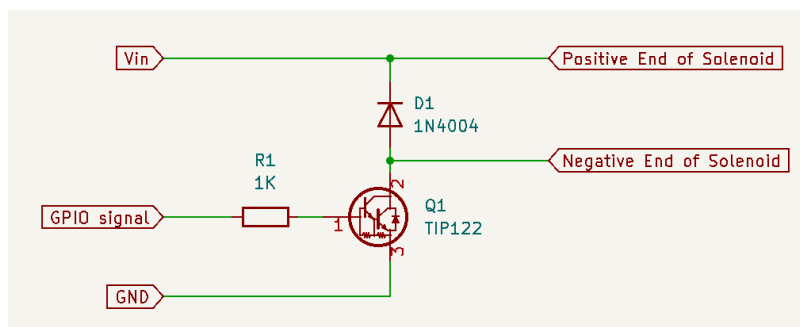


Figure 11: KiCad Schematic of the Solenoid Control Circuit

The proposed system for this project consists of a single water pump and multiple solenoid valves, with each solenoid dedicated to one arm on the robot, enabling precise control over the dispensing process. To facilitate supplying the four solenoid valves from one source, pipe connectors were designed to divert the flow of liquid from the main pump to the respective solenoids. These connectors are either in the shape of a 'T' or 'L' as depicted in Figure 12.



Figure 12: 3D printed pipe connectors used to divert the flow of liquid through the system.

To conserve power and minimize the strain on the pump during periods of non-dispensing, it has been decided to only switch the pump on, a few seconds before the required liquid is to be dispensed. To enable this behaviour the same control circuitry used in the control of the solenoid valves will be implemented to control the power to the pump.

A calibration phase should be implemented to guarantee that the nozzle ejects the herbicide in a precise jet at the required time. This calibration process ensures all the piping is adequately filled with the required liquid and ready to dispense it exactly when the solenoid is activated for dispensing. At the startup of the robot, the water pump should initially run for a few seconds with all the solenoid valves open allowing the herbicide to be fully integrated into the system, this process will also be used to flush out any old herbicide from previous applications. During this startup calibration phase, it is essential to keep the solenoid valves open since the valves also prevent air from escaping the system. In the absence of an escape route for the air within the system, the pumped liquid will not be able to move through the system. By deactivating the solenoid valve, a liquid lock is created between the pump and the input of the solenoid. On the output side of the solenoid valve, it is assumed that the nozzle keyway hole is small enough and will act as a blockade to prevent any liquid from escaping during the closed state of the solenoid valve. This assumption will be verified in the results and discussion section.

3.2.2 Nozzle Design

To obtain a high level of precision multiple designs of different nozzles were investigated, each nozzle is modified off the same external shape with modifications to the internal shape. The collection of nozzles can be seen in Figure 13. Nozzles of various diameters were modelled ranging from 1mm to 2.5mm, along with nozzles with a rectangular keyway as well as a keyway in the shape of a '+'. Multiple designs were produced to test the efficiency of each keyway.

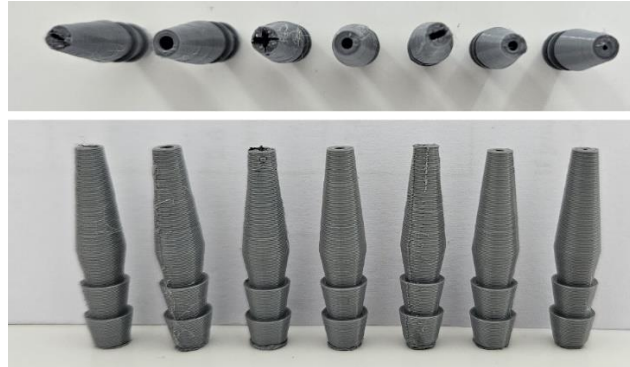


Figure 13: Image showing the different nozzle keyway designs.

To test the accuracy and spray pattern of each of the above nozzles (RQ-02) as well as the optimal mounting height, a comprehensive testing procedure was followed. This process involved writing code to activate the solenoid valve for a 0.5s interval, which was used to control the flow of liquid through the nozzles, in this test water was used within the system. The test rig was fitted with one of the nozzles and mounted at a height of 15cm (Height 1) from the surface, the pulse of water was then sent through the nozzle and the spray pattern was recorded on a piece of paper along with the average diameter of the deposited liquid deposit. Thereafter the test rig was adjusted to a height of 25cm (Height 2) and then 45cm (Height 3) where the same process was followed at each height to determine the effect of the mounting height of the nozzles.

Thereafter nozzle was swapped out to another design and the procedure was repeated to determine the difference in spraying patterns between nozzle key holes. This data is presented in the results section.

3.3 Camera Vision

The next element of the robotic system pertains to the camera vision subsystem, in line with functional requirement RQ-03, which encompasses the system's ability to identify and record data regarding targets. For interpreting the robot's surroundings in this prototype, the chosen component was the Huskylens. This camera module utilises a sophisticated Artificial Intelligence (AI) learning algorithm to identify and track objects across its screen and is easily interfaceable with the Arduino software. This module hosts a two-inch in-plane switching (IPS) screen which enhances functionality, eliminating the need for an external monitor to visualize the data extracted from the camera.

The Huskylens offers multiple functions including, facial recognition, object tracking, object recognition, line tracking, colour recognition, and QR code recognition. This project experiments with object detection and colour recognition features as these would be the most relevant functions to identify a target.

Communication between the Arduino and the Huskylens is established either via Universal Asynchronous Receiver-Transmitter (UART) or Inter-Integrated Circuit (I2C) protocols. This prototype uses I2C to communicate between devices due to its faster transmission speed compared to UART. This allows for real-time image processing, enabling a more robust system.

To train the Huskylens there is a dedicated button on the device used to capture data regarding specific objects/colours. Providing more information under different lighting conditions and angles allows the Huskylens to identify an object more accurately in changing environments. Thus, the quality of information gathered through the learning process is directly correlated with the camera's ability to yield results of high accuracy and reliability.

To test the capabilities of the object detection algorithm employed by the Huskylens, simplified models of both crops and weeds were designed. These models were assembled from a range of identical leaf shapes for both the crop and weed representations and were utilised in the training process of the Huskylens. Coloured stickers were used to train and test the capabilities of the Huskylens colour detection feature.

3.4 Cart Design

This section deals with the physical design of the components and body of the robot required for the final prototype. The conclusions drawn in subsequent sections, based on the above methodology, are applied here. The final body of the robot will be assembled from t-slot 30mm*30mm Aluminium Extrusion bars. This was the chosen material from the body of the robot due to its light weight and its versatility in producing prototypes. The t-slot allows for easy assembly and fixing of the bars together via M6 bolts.

3.4.1 Positioning of Actuation Arms

As determined in the Nozzle Actuation conclusion, the design utilising both the linear and rotational motion was chosen to be implemented. The nozzles should be directed to reach any point within the target region at any time. Selecting the optimal dimensions for the arm length and the positioning of the central pivot point for each arm is an important step. This will determine how many arms need to be implemented in the design.

An increase in the number of arms would increase the efficiency of the robot as these would be able to manoeuvre to the target location much faster as each arm would have a smaller designated target range, although the increase in the number of actuation arms rapidly increases the cost of production of this prototype.

To maximize efficiency, it was determined that the main pivot point of each arm should be positioned along either pivot position 1 (along the bottom edge of the target region) or pivot position 2 (at the centre of the width of the target region), this positioning is further clarified in the results section. Various arm lengths and positions of the pivot point will be simulated in MATLAB software to determine the best configuration of the actuation arms on the robot.

3.4.2 Camera Movement

As concluded in the Camera Vision section, the colour detection feature of the Huskylens will be utilized to identify targets. The camera motion would need to capture data from the full target region of 120cm*40cm. As noted in the conclusion, the optimal mounting height of the camera for this prototype would be at a height of 45cm from the surface, giving a detection region of 58cm*40cm. To capture the full range of data in the target region the camera would have to move in a calculated path to “scan” the environment and generate a target map. The simplest way to achieve this task would be to move the camera along the front of the robot in a stepped manner processing the identified targets within the specific frame and converting this information to a ‘World Coordinate System’.

The devised solution involves a rack and pinion system that will be mounted across the front of the robot and on the camera module to move linearly across the robot. The motor used for this motor is a compact N20 high-power DC motor compatible with a magnetic encoder to track the accurate position of the camera module. This motor is rated at 6V and provides an average speed of 100rpm. Given the substantial length of the target area, the camera movement across the front of the robot should be as fast as possible to decrease the time utilised in the scanning process. To increase the speed of the camera motion module a gear train with a gear ratio of 2.5:1 was designed to translate the motion of the motor to the rack system. The design of the housing unit took into consideration the preexisting keyway within the aluminium bars used to assemble the prototype. The design features two sliders that allow the housing unit to smoothly slide along the keyway, maintaining precise alignment with the rack. The gears, motor and camera module are all mounted onto this sliding housing, which was laser cut from clear Plexiglas. All the above mentioned parts can be seen in Figure 14, and the full assembly of the camera movement system can be seen in Figure 15 using M4 bolts and nuts.

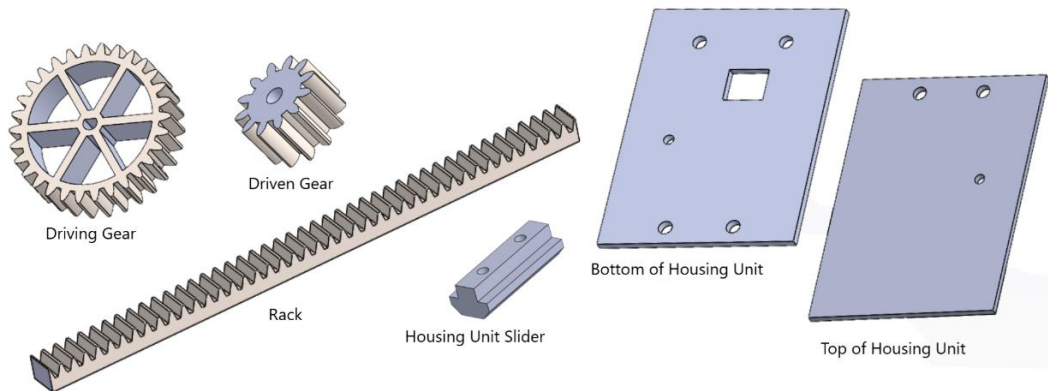


Figure 14: Image showing a collection of 3D modelled parts in SolidWorks of the camera module system.

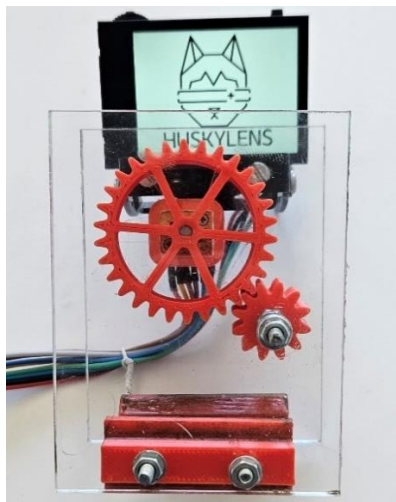


Figure 15: Full assembly of the sliding camera module, including the Huskylens camera.

Integrated into the track of the camera motion, there are 2 push buttons positioned on either end of the track such that when the camera module approaches the end of the rack it triggers the push button signalling to the Arduino that the camera module has indeed reached the start/end position of the rack. This is added as an additional fall back to correct the system with any error the encoder could introduce into the system along its movement across the rack. The addition of this fallback trigger ensures the robot is robust and can correct itself in the case of minor component inaccuracy. The wiring of the pushbuttons can be seen in Figure 16.

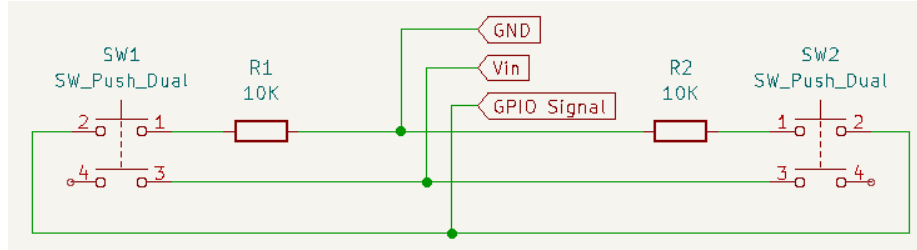


Figure 16: KiCad wiring schematic of the push buttons utilised in the camera movement system.

3.4.3 Linear Movement of Cart

The entire robot must execute precise linear movements in a controlled manner in order to position the array of sprayers and camera system at the designated location. This precise movement of the cart is essential, as the robot must align precisely with the specified point on the 'World Coordinate System'. This is essential since the calculations performed to determine the actuation of each arm rely on the pivot point of the arm being located at a specific location.

The cart is equipped with 4 wheels, two forward driving wheels attached to a motor in the front of the cart along with two wheels 'free wheels' at the back of the cart that get pulled along by the motorized wheels. The motor chosen for this forward driving motion is a 6V DC motor with a no-load speed of 200rpm. Each motor has a torque of 1.92kg.cm and is driven by an H-Bridge motor driver. In addition to the driver, an optical encoder is attached to the back end of the motor to determine the position of the robot.

The two non-motorized wheels are derived from caster wheels, these wheels were stripped of their original housing and a new housing piece was designed and laser cut from hardboard, this housing piece is seen in Figure 17. This housing unit not only holds the wheels in the desired location but also is used as the legs of the robot mounting the main body at the optimal height above the ground. This same housing piece was utilised to hold the front wheels in place to keep some uniformity in the final prototype.

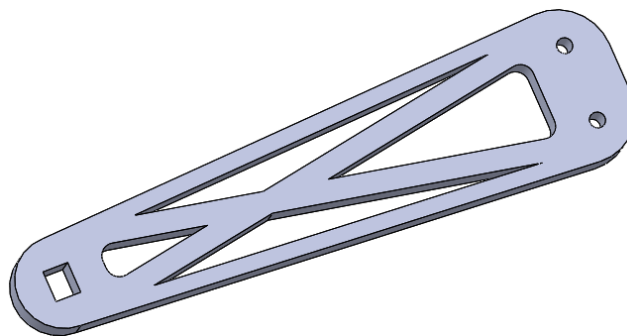


Figure 17: Designed leg of the robot, with mounting holes to hold the wheels in place.

3.5 Code Structure

3.5.1 Obtaining Camera Data

As determined in the Camera Vision section, it was decided to utilize the colour detection feature of the Huskylens for this prototype. After training the Huskylens with the relevant data of the chosen colours, it is left to the Huskylens to do all the complex processing in identifying and representing the identified colours on the screen. Reading data from the Huskylens via I2C provides the user with the height and width of the identified colours present on the screen along with the central x and y coordinates of the identified block.

To simplify the targeting process, the centre coordinates of each target are taken as the only target location and the application of herbicide is directed only to that set of coordinates with the assumption that this is the centre of the weed. The data coming in from the Huskylens is presented in a coordinate system that is centred around its field of view, the origin of the Huskylens is the bottom left-hand corner of the screen. Since the targets are generated from a 'scan' of the environment; stitching together multiple images to develop a full picture of the target region, an algorithm to store an array of targets referenced in a universal coordinate system is developed. The coordinates from the Huskylens can be converted into a universal 'World Coordinate System' by comparing the position of the camera module the moment the image was taken, in reference to the starting end of the robot. The position of the motor can be determined by the magnetic encoder on the motor. Utilising this information, code can be written to adjust the coordinates from the Huskylens coordinate system to the 'World Coordinate System' that is required by the arm actuation code. A flow diagram of how this code should work is presented in Figure 18.

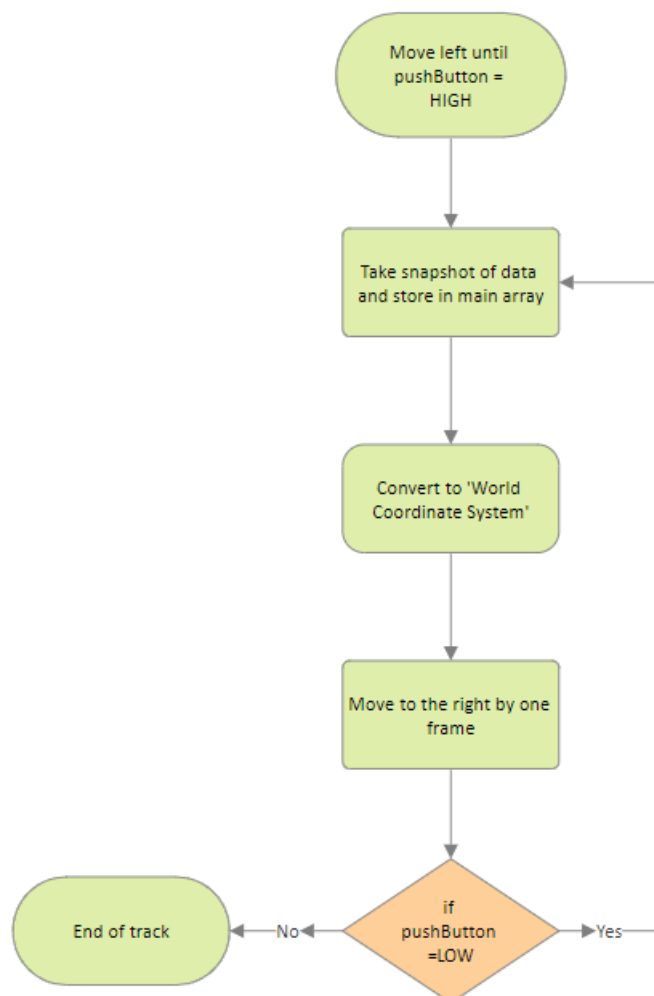


Figure 18: Coding structure to create a target map of the target region.

3.5.2 Allocation of Targets

To calculate how to reach a specific point on the ‘World Coordinate System’, a sorting algorithm and calculations need to be performed on the given set of coordinates. All the computing is done in real-time and processed autonomously on the Arduino IDE. As concluded in the Arm positioning section, the prototype utilises four actuation arms of 25cm each, positioned 30cm apart. The first step of the targeting algorithm sorts all recognised targets from the Huskylens data into 4 arrays. Each array consists of a set of coordinates that are specifically assigned to the arm capable of reaching that designated point. To simplify the allocation process coordinates are categorized off a simplified model of the reachable locations of the arms. A target is allocated to an arm if it is within a 15cm range from the central pivot point of the arm along the x-axis. The simplified target range is illustrated by the coloured blocks overlaid on the reachable target locations plot illustrated in Figure 19.

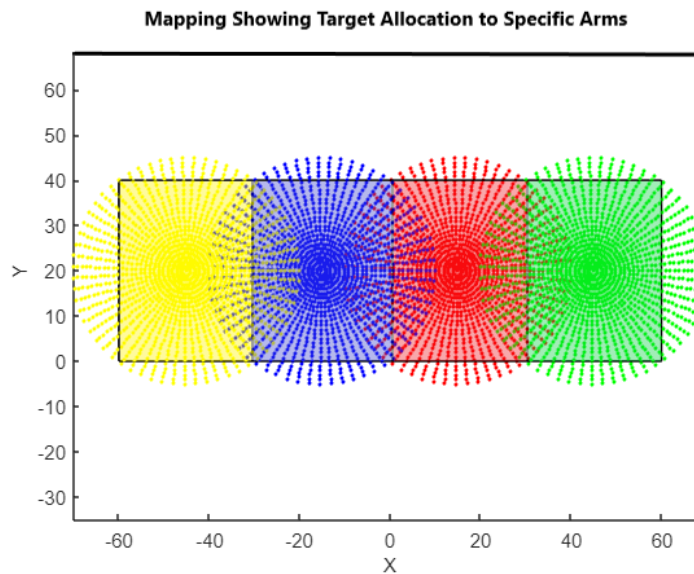


Figure 19: MATLAB simulation showing the allocation of targets, specified by coloured blocks to represent which arm a specific target would get allocated to.

3.5.3 Arm Actuation Algorithm

After the targets are sorted into their respective arms, the next focus will be on the actuation of the arms to these specific positions. In this section, the array of xy coordinates undergoes a conversion process to translate them into a specific number of steps. These steps will be sent to the stepper motors, instructing them on how far to move rotationally and linearly in order to position the end of the actuation arm at the designated location.

The ‘World Coordinate System’ is again converted into a smaller coordinate system, that can be interpreted by each set of arms relative to its pivot point. The targeted coordinate is visualised over a revised coordinate system with designated regions the coordinate could fall under seen in Figure 20. This revised coordinated system has its origin located at the pivot point of the actuation arm to simplify the calculations. Each region on this new coordinate system has its own set of rules to determine the number of steps each motor must move by to position the nozzle at the desired location. Formulas are derived for arm actuation for coordinates that fall in Region One, and slightly adjusted for the other regions using the same methodology of Region One. Regions two, four, six and eight refer to coordinates positioned along either the x or y-axis.

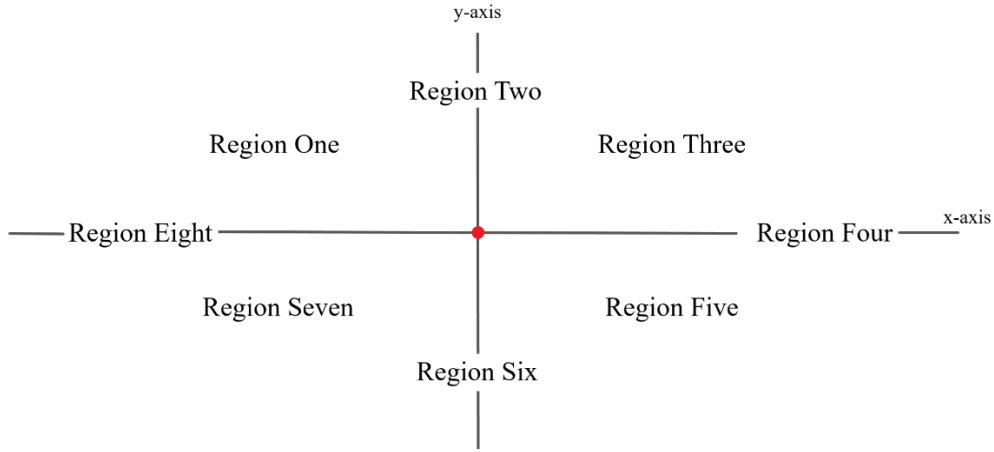


Figure 20: Image showing the different regions a coordinate could fall under relative to the actuation arm pivot point, indicated by the red dot.

As per the data sheet, the motor's complete rotation is equivalent to 2038 steps. This number is manipulated to calculate both the angle necessary for motor rotation and the distance the gear must advance the rack by. Using Figure 21, a set of formulae is derived utilising basic trigonometric formula, to calculate the steps each motor would be required to move by.

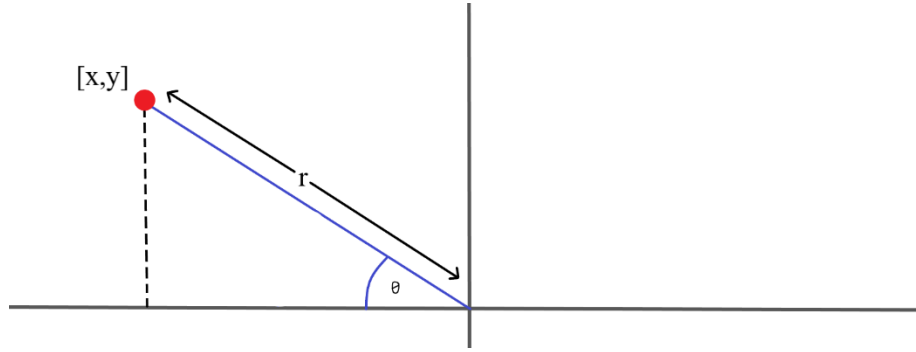


Figure 21: Diagram showing the positioning of a coordinate in region one.

This coordinate falls in region one. The tangent function is utilised to calculate theta as represented in Equation 1.

$$\theta = \tan^{-1} \left(\frac{y_{Coordinate}}{x_{Coordinate}} \right) \quad (1)$$

This angle is then converted to a number of steps using Equation 2. This represents the number of steps the motor responsible for rotational movement of the arm would need to move by. The number 360 is used to convert from degrees to steps.

$$number\ of\ steps = \frac{\theta}{360} \times 2038 \quad (2)$$

Calculating the linear movement of the rack is slightly more complex as it is dependent on the radius of the driving gear. The linear distance the rack needs to move by is calculated using the Pythagorean Theorem, this is shown in Equation 3.

$$r = \sqrt{x^2 + y^2} \quad (3)$$

This value is then converted to steps for the stepper motor using Equation 4. This number now represents the number of steps the linear stepper motor needs to move by. The circumference of the gear is calculated via the formula, $2\pi r_{gear}$. The mean radius of the gear is 1.75cm, this value is substituted into r_{gear} .

$$\text{number of steps} = \frac{r}{2\pi r_{gear}} \times 2038 \quad (4)$$

Transmitting both of these calculated values to the respective stepper motors will enable precise movement of the actuation arm to the intended location. This formula is applied to all the coordinates in the arms' array of targets with slight adjustments to the derived formula for each of the different regions that the coordinate falls in, as mentioned above. These values are stored in the original array assigned to each arm (replacing the xy coordinates). Once the coordinates have been transformed into linear and rotational movement variables, they are sorted into a trajectory for efficient targeting of these points. It has been decided to evaluate the rotational movement variable for each set of coordinates and arrange the targets in ascending order. This approach ensures that the targets are targeted in a logical and efficient sequence. The bubble sort algorithm will be utilised in the code structure to perform this sort. This algorithm iteratively steps through a list and compares the current element with the element, swapping them if necessary. The overall flow diagram of this code can be seen in Figure 22.

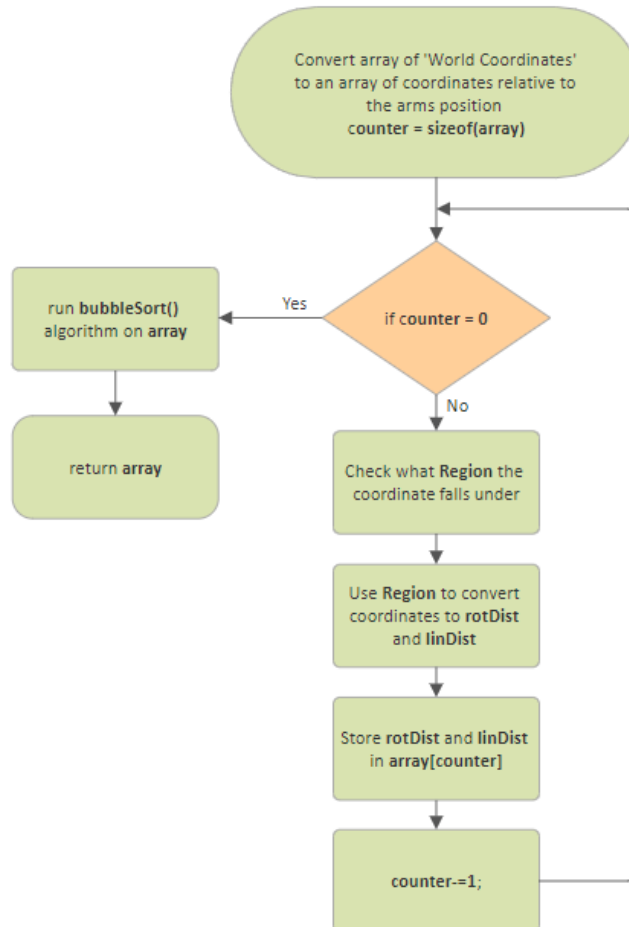


Figure 22: Coding structure to convert 'World Coordinate array' to array of rotational and linear actuation.

3.5.4 Nozzle activation

Once the nozzle is at the desired location a HIGH signal is sent to the control circuitry of both the pump and the respective solenoids to activate the dispensing of the liquid, with a two-second delay between the triggering of the components such that the pump can reach its full force. A snippet of this code is seen in Figure 23.

```
int pumpPin = 3;
int solenoidPin = 4; //These are the output pins on the Arduino we are using

void setup() {
  pinMode(pumpPin, OUTPUT);
  pinMode(solenoidPin, OUTPUT); //Sets the pins as outputs
}

void loop() {
  digitalWrite(pumpPin, HIGH);
  delay(2000); //Wait 2 Seconds for pump to reach full force
  digitalWrite(solenoidPin, HIGH); //Switch Solenoid ON
  delay(1000); //Eject liquid for 1 Second
  digitalWrite(pumpPin, LOW);
  digitalWrite(solenoidPin, LOW); //Switch components OFF
  delay(2000);
}
```

Figure 23: Image showing the code used to activate the pump and solenoid when required.

3.5.5 Full Control Algorithm

The execution path of the code utilized in the final implementation of the robot is outlined in Figure 24, providing a visual representation of the sequential steps in the program's flow.

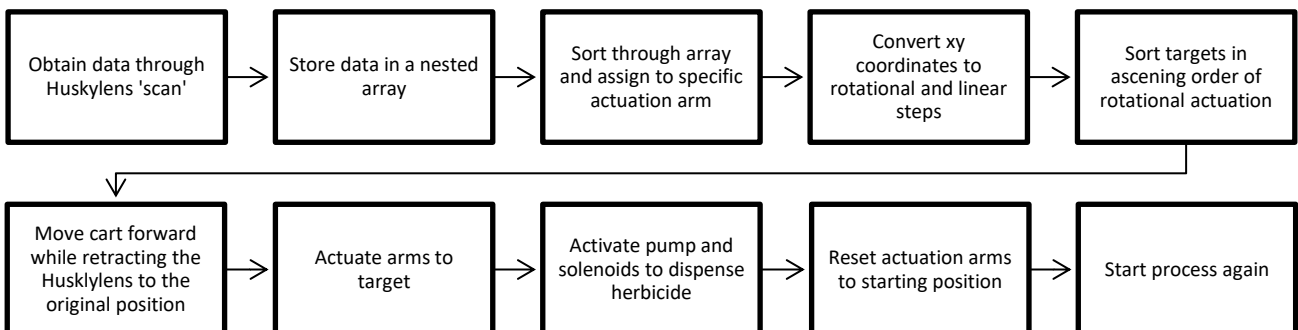


Figure 24: Image showing a simplified structure of the full control algorithm code.

The code developed for this prototype can be found in Appendix A. Table 3 provides a summary of all the defined functions, along with concise explanations indicating the purpose and functionality of each function.

Table 3: Descriptions of functions defined in the control algorithm code.

Function	Description
target()	Takes in xy coordinates and preforms the necessary calculations to obtain the rotational motion and linear motion to actuate the arm to this target.
sortArrayAscending()	Takes in an array of rotational and linear movements and sorts the arrays in ascending order regarding the rotational actuation variable.
sortArrays()	Takes in the main array and handles the entire process of allocation of these coordinates to the correct arm along with calling the other relevant functions to plan the target trajectory of each actuation arm.
initialize()	This function takes in the required stepper motor name and initialises two variables for rotational and linear motion using the provided names.
moveMotors()	Runs a function call to each stepper motor to ensure it is moving to the desired location.
linearForward()	This function controls signals sent to the H-Bridge, controlling the linear motion of the cart.
scan()	This function controls the motion of the camera module in a stepped manner.

3.6 Final Circuitry

The electronics employed in this prototype entail a substantial number of interconnected wires. The simplified wiring schematic for the Arduino Mega is depicted in Figure 25.

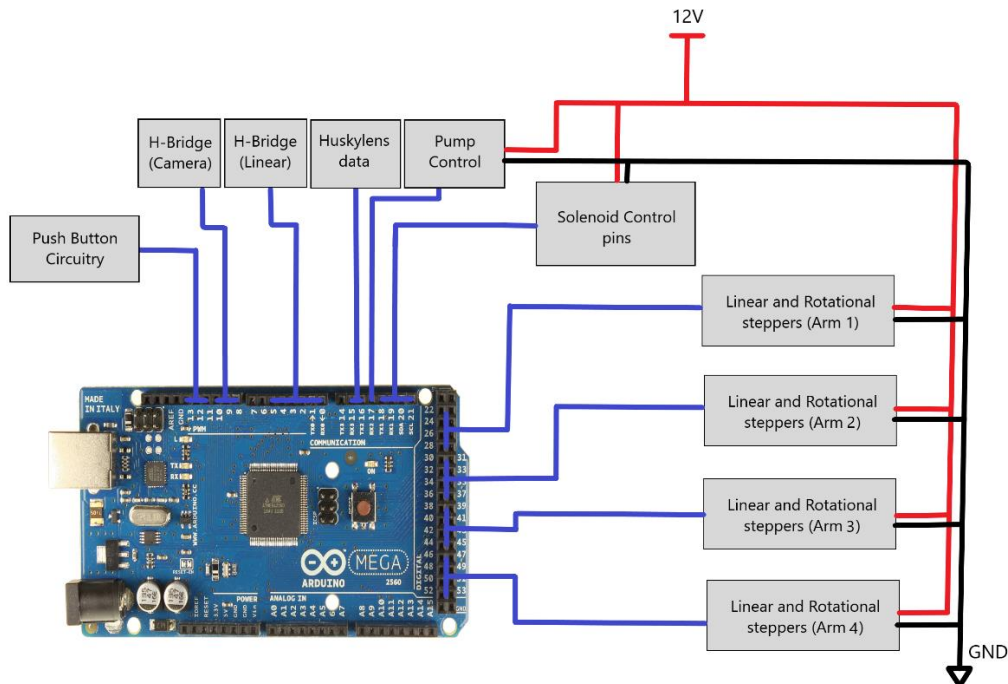


Figure 25: Image showing the wiring schematic of the Arduino board.

3.7 Final Designed Parts

Implementing Design 3, it would be necessary to develop and manufacture several moving components. Due to easy access to 3D printers and laser-cutting machines, most designs were developed with these machines' capabilities and restrictions in mind. The most appropriate material for each design was chosen and produced on the relevant machine.

Each arm was designed in the SolidWorks software and modelled in a simplified part assembly to ensure the pieces interacted with each other as expected and the gears meshed correctly. Since this design utilises multiple motors, the cost of production quickly adds up. The 28BYJ-48 is a cheap and powerful stepper motor, perfect for this application. This stepper motor is powered via a 5V supply and is driven with the ULN2003 driver board.

Both the rotational and linear motion of the actuation arms have their own dedicated stepper motor. Multiple iterations of designs have been experimented with although the final design is only presented in this report, as very small details have been changed between iterations. The linear housing is designed to securely accommodate the motor, ensuring that it is held at the appropriate distance from the keyway to allow smooth passage for the sliding rack. The driving gear is modelled with a module of 1.25 and has 25 teeth. The linear housing unit is affixed to the rotational housing, enabling the linear unit to have full rotational capability. All designed parts can be seen in Figure 26 and the full assembly in Figure 27.

Consecutive arms are positioned on either the short rotational housing or the tall rotational housing, this enables consecutive arms to pass over each other without any obstruction.

Due to limitations of the printer, some components of the arm actuation system have been printed separately and superglue was used to fix them in the desired location. It would be difficult to clean supports off the design in some instances due to the shape of the designed component, where possible the design was adjusted to not require supports during the printing process, and in other cases, they were just printed separately and attached to the main component where necessary.

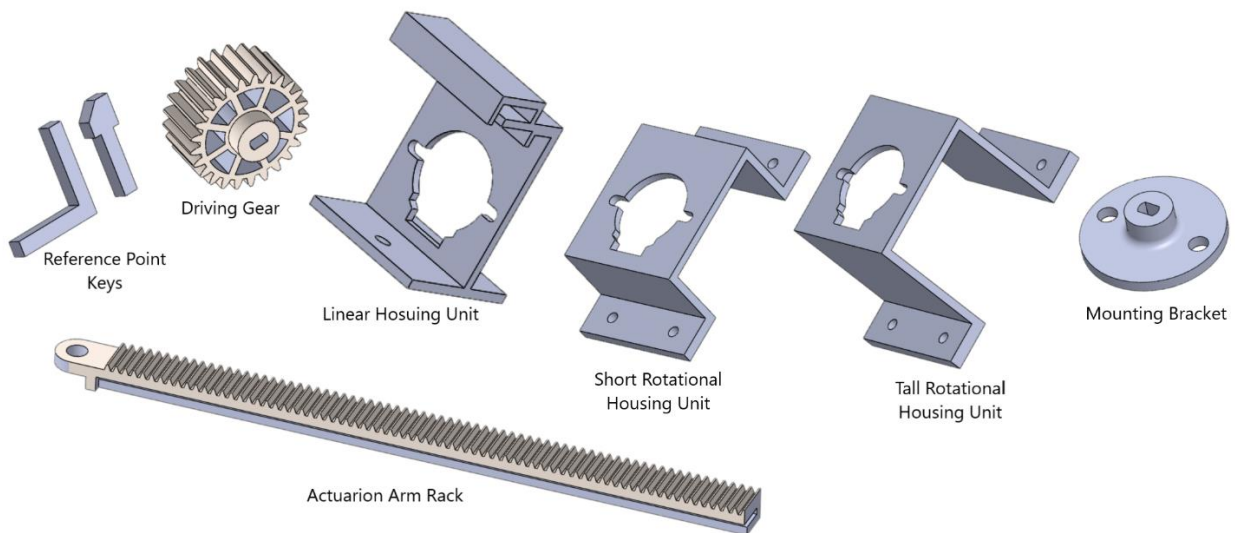


Figure 26: Image showing all parts for the arm actuation system, modelled in SolidWorks.

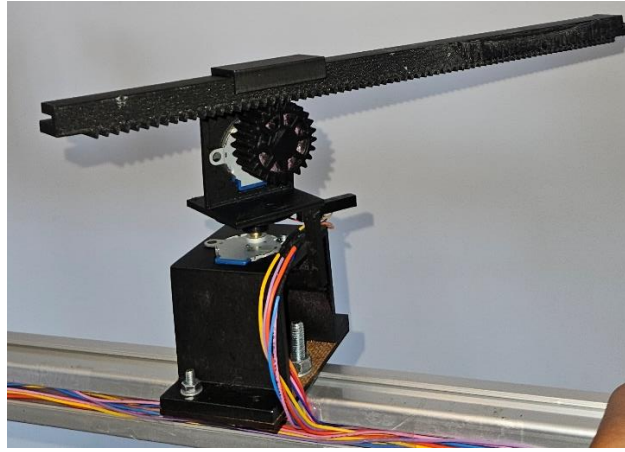


Figure 27: Full assembly of the actuation arm fitted with the stepper motors and mounted onto the prototype.

The stepper motors used in the arm actuation do not utilise encoders to track the position of the arm in the real world, these could be added onto the design but was not done in the case of this prototype due to budget constraints. Not having any additional information about the current position of the motors, would make it difficult to recalibrate the actuation arm to the initial starting point position, to combat this issue the addition of the reference point keys in Figure 26 were added to the design. These keys were adhered to both the rotational and linear housing, which prevents the motor from moving past this point. Preventing the motor from moving beyond this designated point, ensures precise positioning of the motors at the initial starting position. When instructing the motors to return to this position, a slight overshoot can be programmed, knowing that the reference keys will stop the motion at the desired location. This approach enhances the accuracy and reliability of the system.

The final assembly of the prototype is shown in Figure 28 below and a complete budget breakdown of this prototype can be found in Appendix B. In the Figure the following is labelled: A is the microcontroller, B highlights one of the actuation arms, C is the camera movement system including the Huskylens, D is the pump for liquid dispensing and E highlights one of the forward driving wheel.

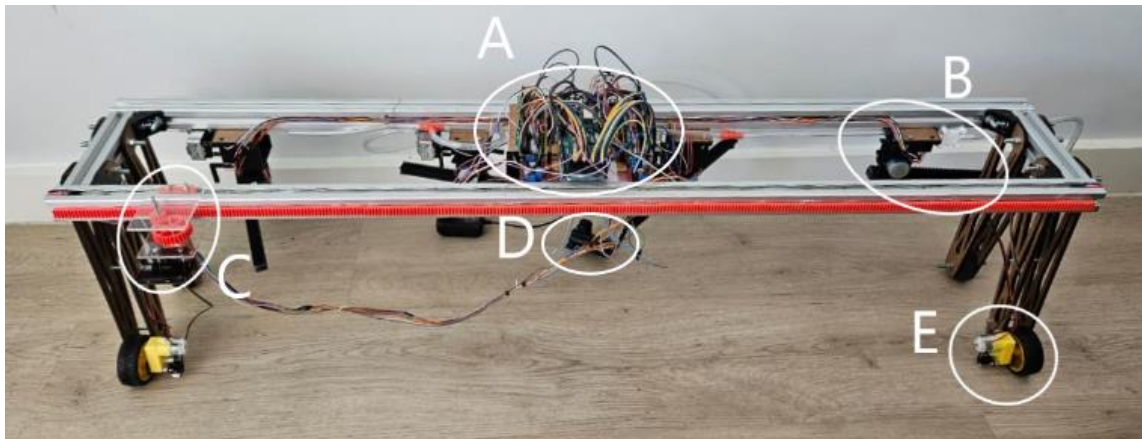


Figure 28: Image showing the full assembly of the precision herbicide sprayer prototype. (A) Microcontroller, (B) Actuation Arm, (C) Camera Movement System, (D) Liquid Dispensing pump and (E) Motorized Wheel.

4. Results

4.1 Nozzle Actuation

To decide which design to continue the prototyping process with, simulations and physical tests were completed to assess the viability of each design presented in the methodology, with the goal of functional requirement RQ-01 in mind.

Below shows a MATLAB simulation of the reachable target locations of designs two and three (Figure 29). The simulated results make use of two arms each measuring 20cm. Analysing the reachable target locations in Figure 29(a), it is noted that the design would be able to reach the same target location using multiple different configurations. The actuation arms could also fold back very compactly to avoid collision with consecutive arms mounted nearby. In Figure 29(b) the simulated results make use of a 40cm arm, it is evident that to reach a specific location, there is only one viable path available for targeting that point.

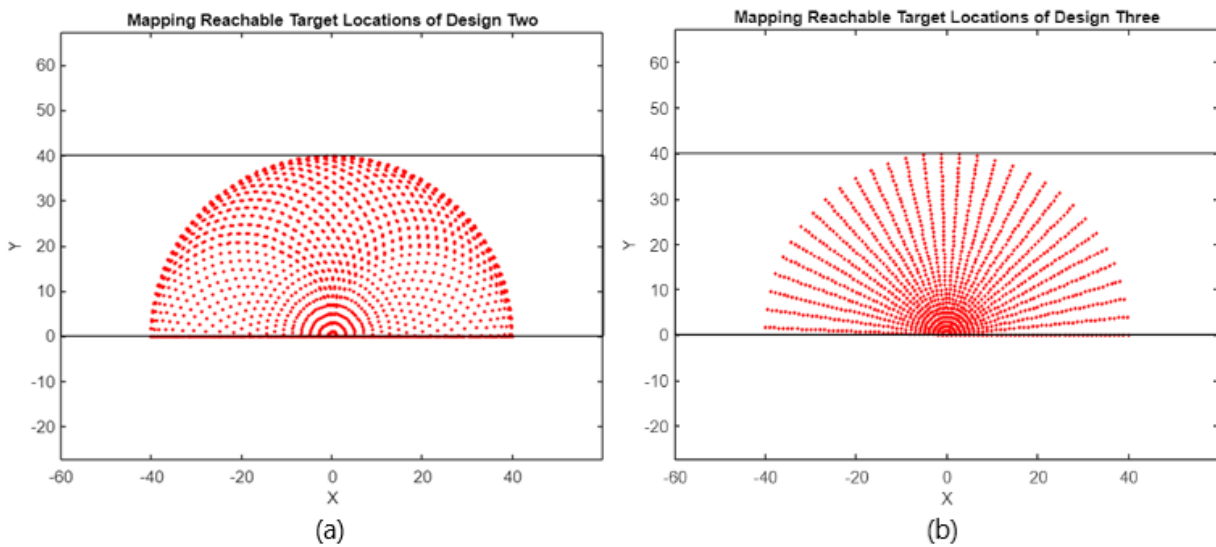


Figure 29: MATLAB simulations of reachable target locations of Design Two (a) and Design Three (b).

4.1.1 Nozzle Angle Test

To test the viability of design one the following test was completed. Figure 30 below shows the effect of a change in angle in the deposited liquid. The 1mm diameter keyway nozzle was mounted at a height of 15cm from the surface and a pulse of water was sent through the nozzle as outlined in the methodology. Initially, the nozzle was mounted perpendicular to the surface, to investigate the effect of the change in the angle of the nozzle, thereafter the nozzle was adjusted by 15° and the process was repeated, and the results are presented below.

This was done 5 times to get the maximum angle the nozzle would have to move which is 60° .

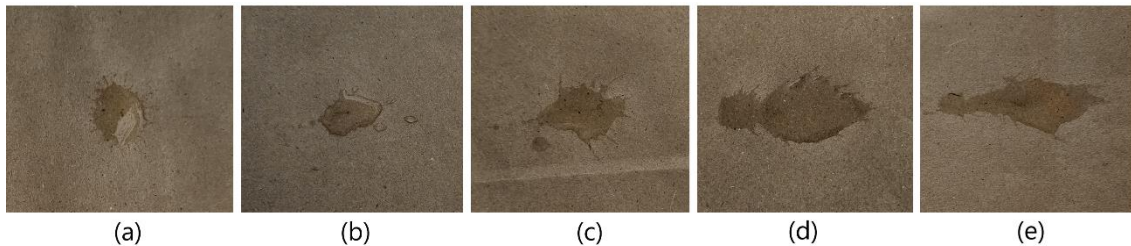


Figure 30: Image showing the change in the pattern of the deposited liquid with a change in the angle of the nozzle. (a) shows the nozzle mounted at the central position of 0° , (b) at 15° , (c) at 30° , (d) at 45° and lastly (e) at 60° from the central position.

It can be seen from Figure 30 that as the nozzles' tilt angle increases there is a direct effect on the pattern of the deposited liquid on the surface. At the maximum angle of 60° , there is a significant splash width produced by the nozzle. There were no visible splashes created by satellite drops between the pivot point of the nozzle and the deposit site of the liquid. The average width of the deposited liquid along with its respective nozzle angle is summarized in Table 4.

Table 4: Showing the change in the average width of the deposited liquid relative to the change in nozzle angle.

Nozzle Angle	Average Width of the Deposited liquid
0°	1.6cm
15°	2.7cm
30°	3.4cm
45°	5.6cm
60°	7.5cm

4.2 Arm Positioning

In the conclusion section, it was determined that Design 3 was chosen for the final prototype. The subsequent results section builds upon this decision to further progress with the testing process. The specific dimensions and number of arms required to target the desired target region can now be determined given this information. Figure 31 shows a collection of MATLAB simulation plots showing the reachable locations of various arm dimensions with their main pivot point centred at pivot point one (along the edge of the target region). The arm length cannot be too long as when the arm is fully extended the full weight of the arm would need to be supported by only one end.

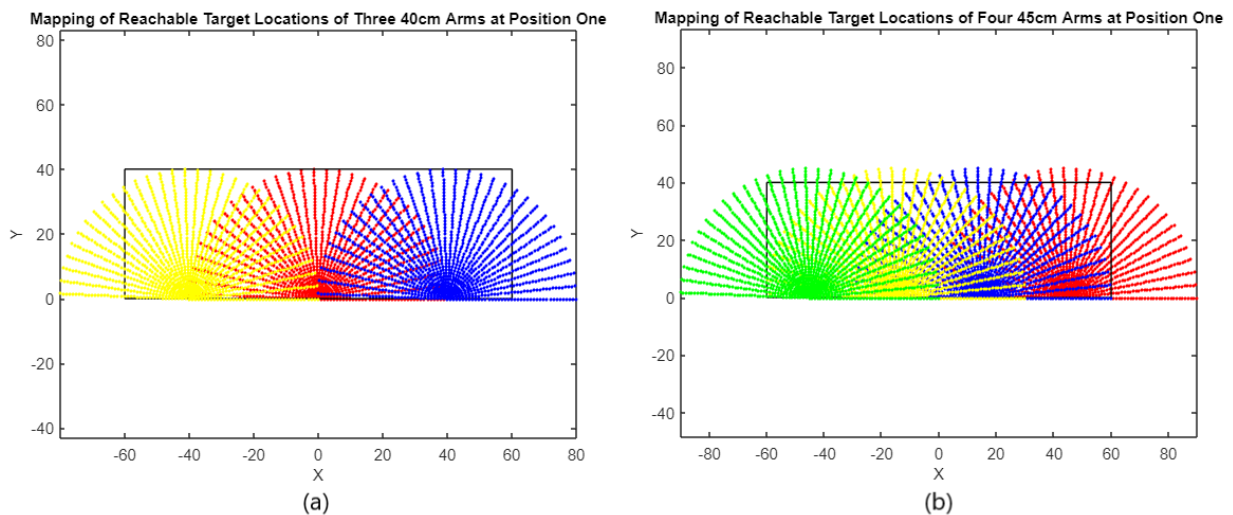


Figure 31: MATLAB simulations showing a mapping of reachable target locations of Design 3, utilising various arm lengths positioned at pivot point one, which is along the edge of the target region. Plots are labelled above the respective plots.

The length of the arms mounted at position one is notably long as these need to span they full width of the targeted region, these arms are only required to move by 180° .

Figure 32 shows plots of arm positions centred at pivot point position two, this position allows many more options on how to cover the target region. Figure 32(a) and (b) utilise a 20cm arm, there are ample dead spots present in this configuration and it requires many arms to eliminate these dead spots. Figure 32(c) has a few dead spots but is easily eliminated by the introduction of one more set of arms as seen in Figure 32(d). Figure 32(e) provides a good coverage of the target region with the 30cm arm although the arms do operate for a large portion of its range outside of the target region and require a significantly long arm.

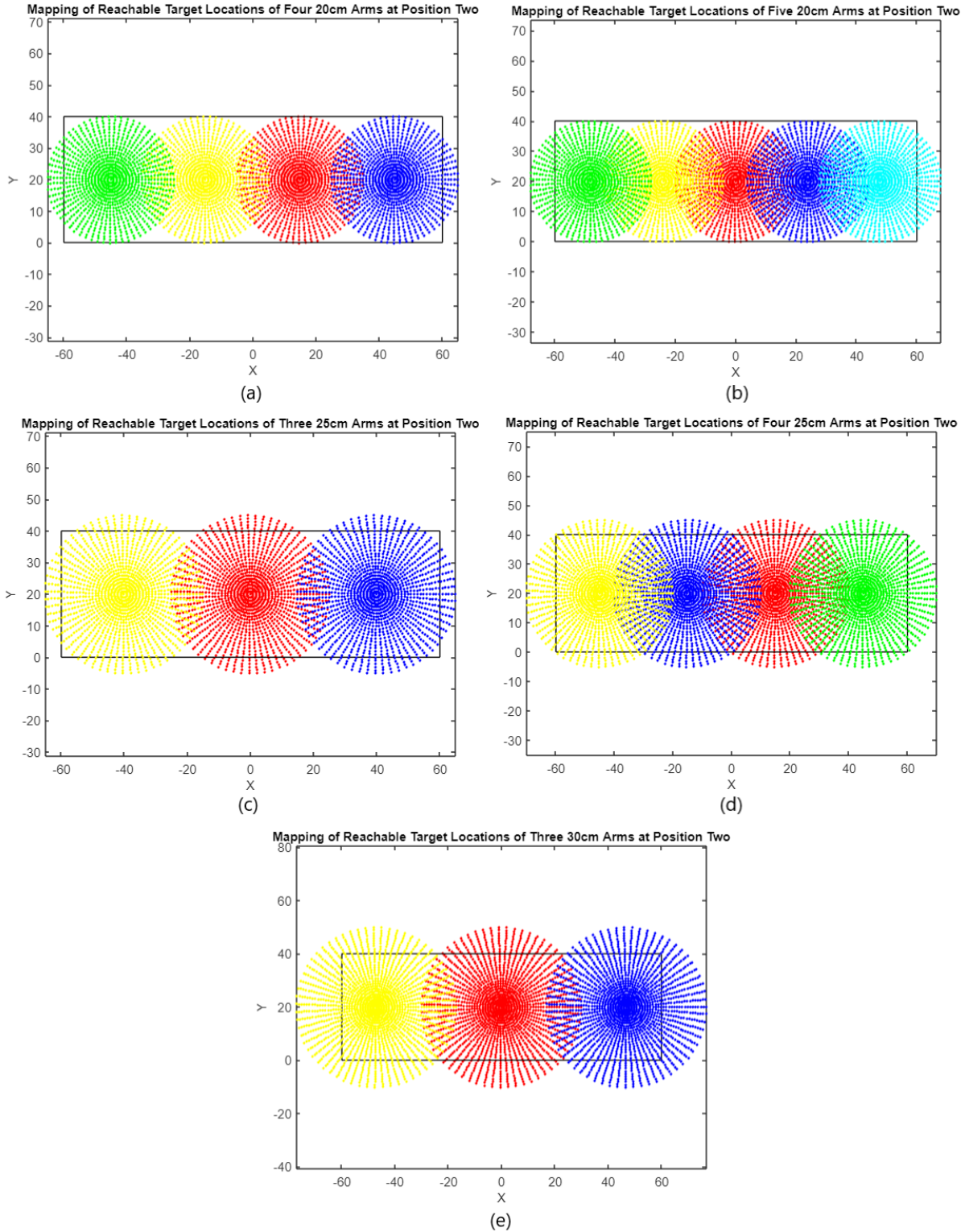


Figure 32: MATLAB simulations showing a mapping of reachable target locations of Design 3, utilising various arm lengths positioned at pivot point two, which is along the central line of the target region. Plots are clearly labelled above the respective plot.

4.3 Nozzle Height and Design Test

To meet functional requirement RQ-02, as outlined in the methodology section, the various nozzle designs underwent evaluation through a testing process where they were subjected to a pulse of water. The resulting spray patterns were recorded and are visually represented in Figures 33-29 below.

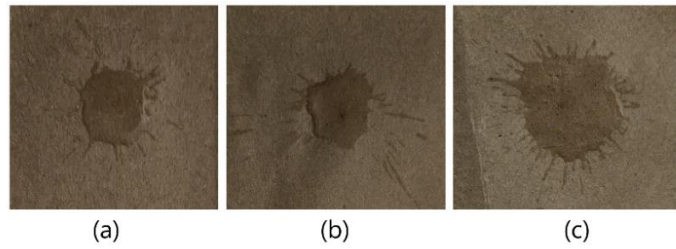


Figure 33: Spraying pattern of a 1mm diameter keyway in the nozzle. (a) Nozzle mounted 15cm from the surface with an average splash diameter of 1.7cm, (b) Nozzle mounted 25cm from the surface with an average splash diameter of 2.6cm, (c) Nozzle mounted 45cm from the surface with an average splash diameter of 3.4cm.

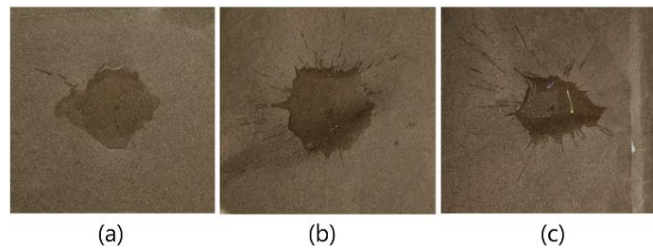


Figure 34: Spraying pattern of a 1.5mm diameter keyway in the nozzle. (a) Nozzle mounted 15cm from the surface with an average splash diameter of 3.5cm, (b) Nozzle mounted 25cm from the surface with an average splash diameter of 4.4cm, (c) Nozzle mounted 45cm from the surface with an average splash diameter of 5.5cm.

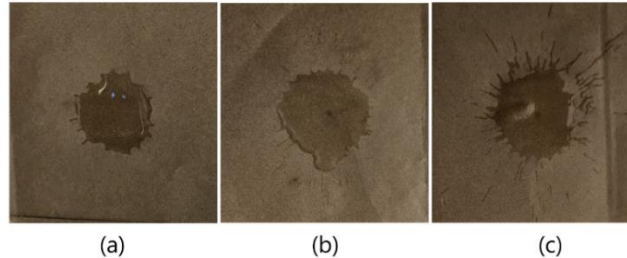


Figure 35: Spraying pattern of a 2mm diameter keyway in the nozzle. (a) Nozzle mounted 15cm from the surface with an average splash diameter of 4.5cm, (b) Nozzle mounted 25cm from the surface with an average splash diameter of 5.5cm, (c) Nozzle mounted 45cm from the surface with an average splash diameter of 6.6cm.

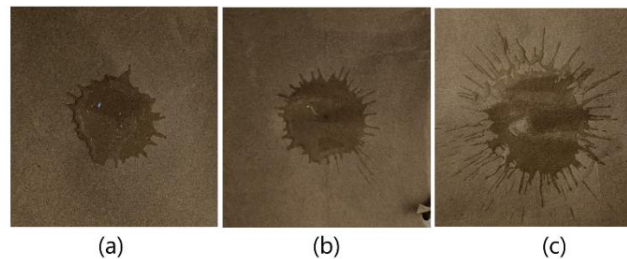


Figure 36: Spraying pattern of a 2.5mm diameter keyway in the nozzle. (a) Nozzle mounted 15cm from the surface with an average splash diameter of 5.6cm, (b) Nozzle mounted 25cm from the surface with an average splash diameter of 6.5cm, (c) Nozzle mounted 45cm from the surface with an average splash diameter of 7.4cm.

Figures 33 - 36 depict the spray patterns observed from nozzles equipped with a circular keyway. It was noted in the above results that there was a positive correlation identified between the height at which the nozzle was mounted above the surface and the average splash diameter of the deposited liquid. It can be seen in these Figures that as the height increased so did the degree of splashing in the deposited liquid. In addition to an increase in splashing, the overall diameter of the deposited liquid also increased with the increase in the mounting height of each nozzle.

Figures 37 and 38 show the splash pattern of the rectangular keyway. In Figure 37 it can be seen that as the mounting height of the nozzle increased the deposited liquid tended to spread out much more. Figure 38 shows a trend of the deposited liquid becoming more circular as the mounting height increases. In addition to this, the least amount of splashing was present at the mounting height of 25cm.

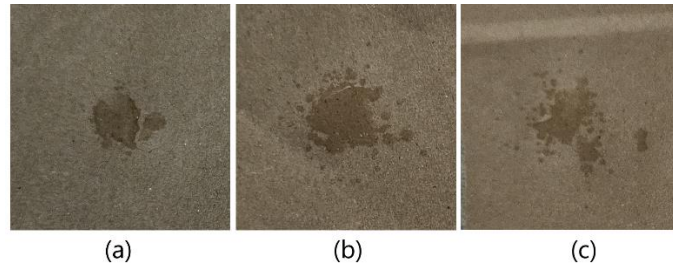


Figure 37: Spraying pattern of a rectangular keyway in the nozzle (2.4mm*0.4mm). (a) Nozzle mounted 15cm from the surface with an average splash diameter of 1.4cm, (b) Nozzle mounted 25cm from the surface with an average splash diameter of 1.7cm, (c) Nozzle mounted 45cm from the surface with an average splash diameter of 2.5cm.

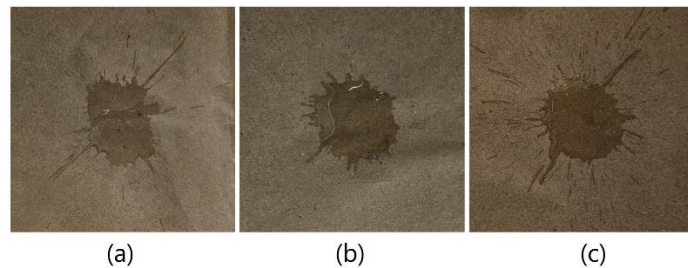


Figure 38: Spraying pattern of a rectangular keyway in the nozzle (2.4mm*0.8mm). (a) Nozzle mounted 15cm from the surface with an average splash diameter of 3.5cm, (b) Nozzle mounted 25cm from the surface with an average splash diameter of 4.6cm, (c) Nozzle mounted 45cm from the surface with an average splash diameter of 5.4cm.

The '+' designed keyway produced the most irregular splash pattern and caused significant splashing due to satellite drops forming while ejecting the liquid from the nozzle. This can be seen in Figure 39, it is also noted that there is no central deposit of liquid, the liquid is deposited in an irregular pattern on the surface.

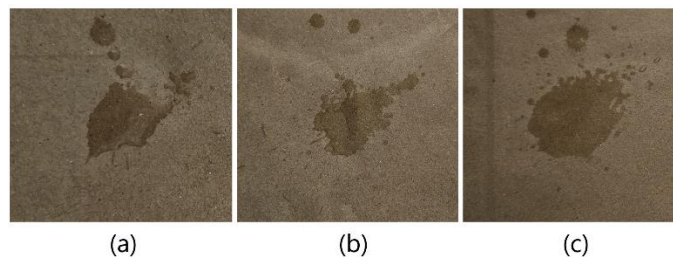


Figure 39: Spraying pattern of '+' keyway in the nozzle. (a) Nozzle mounted 15cm from the surface with an average splash diameter of 2.6cm, (b) Nozzle mounted 25cm from the surface with an average splash diameter of 3.7cm, (c) Nozzle mounted 45cm from the surface with an average splash diameter of 4.6cm.

The above information regarding the change in size of the deposited liquid is summarized in Table 5 to easily compare the results.

Table 5: Showing the effect of mounting height of different nozzles and the average diameter of the deposited liquid.

Nozzle Keyway Design	Average Diameter of Deposited Liquid from Height One (15cm)	Average Diameter of Deposited Liquid from Height Two (25cm)	Average Diameter of Deposited Liquid from Height Three (45cm)
1mm Diameter	1.7cm	2.6cm	3.4cm
1.5mm Diameter	3.5cm	4.4cm	5.5cm
2mm Diameter	4.5cm	5.5cm	6.6cm
2.5mm Diameter	5.6cm	6.5cm	7.4cm
Rectangular (2.4mm*0.4mm)	1.4cm	1.7cm	2.5cm
Rectangular (2.4mm*0.8mm)	3.5cm	4.6cm	5.4cm
‘+’ Design	2.6cm	3.7cm	4.6cm

4.4 Herbicide Volume test

To develop an accurate answer on how much liquid is dispensed through the system, a volume test was carried out. This test involved pulsing a just of water through the system and measuring the volume of the expelled liquid from the nozzles. The solenoid was triggered to turn on for one second and a syringe was held at each nozzle to measure the volume of liquid released. This test was carried out 3 times and the average of the readings were recorded in Table 6. This test was carried out for each nozzle as the distance the liquid would have to travel to each solenoid is different. Solenoid 1 is positioned on the far-left side of the robot and Solenoid 4 is located at the far right of the robot.

Table 6: Showing the average volume of liquid deposited from each solenoid.

Solenoid Number	First Volume Test	Second Volume Test	Third Volume Test	Average of the Volume Tests
Solenoid 1	1.4ml	1.3ml	1.6ml	1.433ml
Solenoid 2	1.1ml	1.4ml	1.5ml	1.333ml
Solenoid 3	1.4ml	1.6ml	1.3ml	1.433ml
Solenoid 4	1.4ml	1.6ml	1.7ml	1.566ml

The above results indicate that the liquid dispensing system has some imprecision, with a maximum range deviation of 0.6ml observed across the individual tests and a deviation of 0.233ml across the average of the volume tests.

4.5 Nozzle Accuracy Test

Given that the nozzle accuracy is of pivotal significance to this project, this aspect has been given special attention. Substantial efforts have been made towards ensuring this prototype yields reliable results to fully satisfy the functional requirement RQ-02.

4.5.1 Rotational Accuracy Test

To assess the rotational accuracy of the actuation arms, a set of specific angles were transmitted to the stepper motor controlling the rotational motion of the arm. This command was done multiple times to evaluate both the accuracy and precision the actuation arm. The outcome of this test is presented in Table 7 below.

Table 7: Showing the results of the accuracy test on the rotational arm actuation.

Target Angle	First Iteration	Second Iteration	Third Iteration	Fourth Iteration	Fifth Iteration
45°	45.0°	45.0°	45.0°	45.1°	45.0°
135°	135.0°	135.0°	135.1°	135.1°	135.0°
225°	224.8°	225.0	225.2°	224.9°	225.1°
315°	315.0°	314.2°	315.3°	315.1°	314.7°

As observed in the table above the rotational movement was able to navigate smaller angles with high precision and accuracy, differing at most by 0.1°. As the motor attempted to navigate to the larger angles there was a slight deviation in precision and accuracy. The motion yielded more accurate results for smaller angles.

4.5.2 Linear Accuracy Test

To assess the linear accuracy of the actuation arms, the same method used to test rotational accuracy was implanted. A series of specific distances were transmitted to the stepper motor controlling the linear motion of the arm. This command was also executed multiple times to test the precision of the actuation arms. The outcome of this test is presented in Table 8 below.

Table 8: Showing the results of the accuracy test on the rotational arm actuation.

Target Distance	First Iteration	Second Iteration	Third Iteration	Fourth Iteration	Fifth Iteration
5cm	5.00cm	5.05cm	5.00cm	5.00cm	4.95cm
10cm	9.95cm	10.10cm	10.00cm	9.90cm	10.00cm
15cm	15.05cm	15.10cm	15.00cm	14.90cm	14.95cm
20cm	20.25cm	20.20cm	19.85cm	19.95cm	20.10cm
25cm	25.15cm	25.40cm	25.20cm	24.75cm	25.05cm

As observed in the table above the linear arm action performed well. As noted in the rotational accuracy test, similar results can be seen in the linear test. When targeting shorter distances, the motor had a higher accuracy rate and got slightly worse when targeting longer lengths.

4.5.3 Combined Test (single target)

This test was conducted to evaluate the accuracy of the combined rotational and linear actuation of an arm in accurately targeting a point within the coordinate system with the activation liquid dispensing. A specific coordinate was transmitted through the system, and the arms were actuated to move to this designated point indicated by the + in Figure 40. This procedure was repeated three times for each target to assess accuracy. Figure 40 presents a representative set of results from this examination.

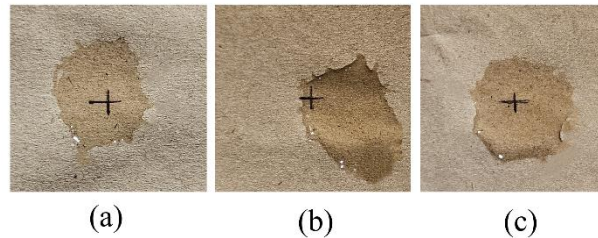


Figure 40: Images showing the accuracy of the system when targeting a single point.

As seen in Figure 40, the deposited liquid was not always perfectly centred over the targeted coordinate, although the coordinate is consistently covered by a significant portion of the deposited liquid. It is also noted that the degree of splashing in the full assembly was reduced as compared to the results noted in the Nozzle Height Test.

4.5.4 Combined Test (multiple targets)

In a second combined test, a set of random coordinates spanning the entire target region was sent through the sorting algorithm and converted to rotational and linear steps for each of the actuation arms. These commands were then executed to test the ability of the sorting algorithm to handle multiple targets meeting functional requirement RQ-03.

The sorting algorithm was able to categorize the provided set of coordinates to the correct arms and generate the appropriate values to transmit to the stepper motors relative to the actuation arms' position on the full assembly of the prototype. This test yielded results consistent with those achieved when targeting a single coordinate with one set of arms as illustrated above in Figure 40.

4.6 Camera Vision

Another aspect of function requirement RQ-03 involves the identification of different targets. To enhance the accuracy of the system, the learning process was completed while varying the lighting conditions. It was found that varying the lighting conditions enabled the camera to identify objects/colours with greater precision, the system was minimally affected by various lighting conditions.

4.6.1 Object Detection

Figure 41 displays some images captured by the Huskylens, positioned at a distance of 20cm from the target while attempting to differentiate between a weed (ID1) and a crop (ID2). It's noted that the object detection block maintains a fixed size and occupies a substantial portion of the screen. In

41(a) and (b) the object has been identified correctly under either object ID1 or ID2. However, Figure 41(c) presents a frame where both the weed and crop targets appear in the same frame. When both the weed and crop are present in one frame, the identified object ID fluctuates between ID1 and ID2. Figure 41(c) presents a unique outcome, the Huskylens registers an object ID of ID1, even though there is no target present in the frame. This behaviour appears to be a default setting of the Huskylens as when the background changed the camera produced a constant identification of object ID1.

Despite training the Huskylens with a specific leaf configuration representing the crop/weed, it was able to identify various models of both the crop/weed each with a unique leaf configuration.

Furthermore, it's worth mentioning that the Huskylens solely provides the user with the detected ID code, without supplying any additional information about the precise position of the target within the frame.

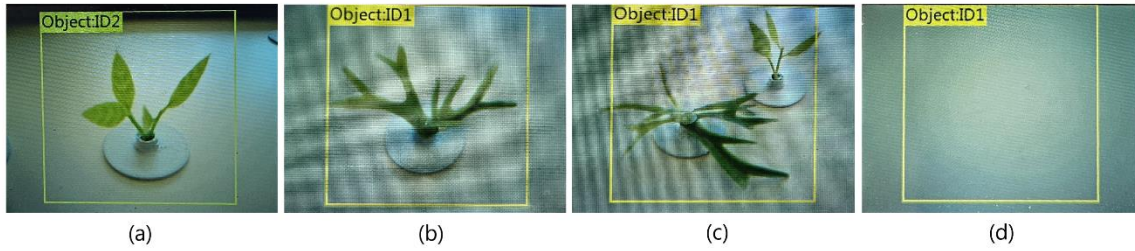


Figure 41: Images from the Huskylens object detection setting identifying the difference between crops and weeds; (a) correct identification of a crop, (b) correct identification of a weed, (c) inaccurate identification of objects given that there are two objects in one frame, (d) incorrect identification of an object.

4.6.2 Colour Detection

The Huskylens was trained with green (ID1) and pink (ID2) stickers to test its colour detection capabilities. In Figure 42(a) the camera was mounted directly above the coloured stickers representing the crop/weeds at a height of 25cm from the surface. This produced a viewable field range of 20cm*13cm per frame. The Huskylens was able to identify targets with accuracy and efficiency, even when multiple targets were present in a single frame.

To cover the entire length of the target region (120cm), the camera would have to be mounted at a height of 100cm from the surface. At this height, the camera was unable to identify any targets, regardless of lighting conditions. In Figure 42(c), the camera was mounted at a height of 65cm from the surface. At this height, the camera managed to identify some targets, although a large portion of the targets in the frame remained undetected.

Figure 42(b) shows an image captured from the Huskylens with the camera mounted at a height of 45cm from the surface, resulting in a field range of 58cm*40cm. At this height, the camera was able to identify all targets with remarkable accuracy and speed, even under varying lighting conditions.

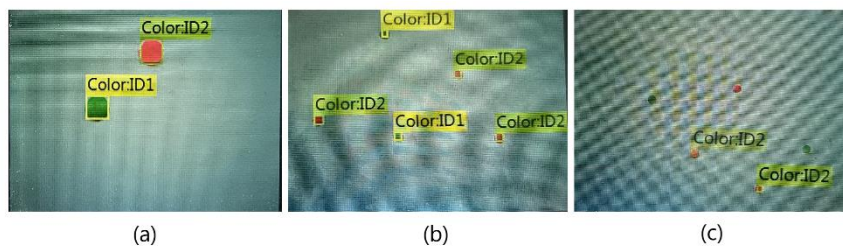


Figure 42: Images utilising the Huskylens colour detection function identifying coloured stickers with the camera mounted at different heights, (a) camera mounted at a height of 25cm from the surface, (b) camera mounted at 45cm from the surface, (c) camera mounted at 65 cm from the surface.

In this specific camera setting, it is possible to extract both the width and length of each target from the data. Additionally, the central x and y coordinates of each target can also be extracted from the data, this coordinate is presented in relation to the Huskylens' screen coordinate system.

5. Discussion

5.1 Nozzle Actuation

Design two offers a versatile configuration in targeting specific points from multiple angles, this enables a robust trajectory path as the actuation arm could be configured in multiple configurations to reach a specific location. However, mounting the second actuation stepper motor at the end of the first link of the arm adds extra weight to the end of the first link, thus creating an unbalanced force around the main pivot point. This could lead to an excess amount of stress on the stepper motor, potentially impacting its performance and ability to move the actuation arm.

On the other hand, while design three is limited to approaching a specific point via a single path, it has all the heavy components, particularly the stepper motors, positioned at the main pivot point. This design choice minimizes the weight of the extendable actuation arm, as only the arm and nozzle will be extended. This design prioritizes the stepper motors' performance, which is a crucial factor in ensuring the system's accuracy and reliability.

Analysing the results of the test for Design One, investigating the effect of the change in angle in the deposited liquid, there was a significant increase in the size of the deposited liquid as the nozzle tried to hit targets further away from the central pivot point of the mounted nozzle. This resulted in very large deposits of liquid outside of the target region. The absence of satellite drops could be due to the high pressure provided by the pump on the input end of the solenoid.

5.2 Arm Positioning

As depicted in Figure 30, positioning the pivot point of the actuation arms at position 1 severely affects the allowable length of the actuation arms. This pivot point placement necessitates extremely long arms to cover the full target region. These longer arms introduce a significant amount of stress on the pivotal motor as the arm is extended.

Figure 31 illustrates that as the length of the actuation arm decreases the total number of arms required to fully cover the target region increases, this in turn increases the cost to produce the prototype.

Therefore, it is important to select a configuration with the shortest possible arm length and the fewest number of arms to minimize the unbalanced forces of the central pivot point and to optimize production costs. The 20cm arm in Figure 31(a) and (b) would require an excessive number of arms to gain proper coverage of the target region. This is because the maximum length of each arm is equivalent to half the width of the target block, this design would require the pivot point of each arm to be positioned extremely close together to eliminate any potential dead spots within the target region.

5.3 Nozzle Height and Design Test

In the results section it can be seen that across all nozzles' designs, the increase in mounting height above the surface resulted in an increase in the splashing present in the deposited liquid along with an increase in the average diameter of deposited liquid. This increased splashing is a direct consequence of the water having to travel a longer distance before making contact with the surface. The longer travel distance of the liquid leads to an increased velocity upon impact, thus resulting in a significant splashing effect.

In Figure 37, the rectangular keyway of 2.4mm*0.8mm mounted at a height of 25cm from the surface produced an outlier from previous results as at this height the least splashing occurred for this specific nozzle. In all other tests, the least splashing generally occurred at the shortest mounting height of each nozzle. Thus, for this rectangular keyway, the optimal mounting height would be 25cm from the surface. The rectangular keyway shown in Figure 36, also presented an interesting outcome in the results section. The deposited liquid formed an irregular spray pattern. This inaccuracy could be a direct effect of the capabilities of the 3D printer used. The keyway consisted of very small dimensions, rendering the 3D print very intricate, slight inaccuracies within the keyway could have resulted in the irregular spray patterns.

While these results were obtained using water, it is noted that different liquids would yield slightly varied splashing patterns as noted in the works of [17]. However, the trends observed in these results using water can still be considered valid. If similar tests were conducted with another liquid, we would expect to see a similar trend in the changes in splashing patterns between different tests. The main difference would likely be the degree of change in splashing from one test to the next, based on the specific properties of the new liquid used.

5.4 Herbicide Volume Test

As evident in the results section, there was no clear trend in the volume of liquid dispensed relative to the distance at which the solenoid was mounted from the central pump. In addition to this, the results indicate a lack of consistency in the dispensing of liquid from each solenoid. This variability in the dispensed liquid could be due to the pump's pressure not being regulated. Additionally, the pump requires a few seconds to reach its maximum pressure. It's worth noting that the pump utilised is not designed for the precise application of pressure, and slight fluctuations in the output pressure could be the reason for these variations in liquid dispensing.

5.5 Nozzle Accuracy Test

5.5.1 Rotational Accuracy Test

The results obtained from the rotational actuation test presented a high level of accuracy in rotational actuation. This indicates that the rotational movement mechanism is functioning effectively.

The addition of reference point keys in the design of the actuation arms serves as a crucial fail-safe measure. This fallback mechanism significantly enhanced the overall robustness and reliability of the robot's design, providing an added layer of security against potential disruptions in operation of the arm actuation. However, due to the thickness of the key, it prevents the actuation arm from completing a full rotation. The actuation arms cannot rotate to angles greater than 353° .

This leaves a triangular dead zone of roughly 37.5cm^2 per actuation arm. Given the entire targeted region and the placement of the arms at 30cm intervals, the consecutive actuation arm can partially cover the dead zone created by the adjacent actuation arm. This positioning of the pivot points of the arms covers a large portion of the dead zone created by the reference key reducing the untreated dead zone area to 1.53cm^2 per arm and 6.14cm^2 in total. Thus, the coordinates that fall under this region must be assigned to the adjacent actuation arm. This dead zone is an extremely small area given that the total targeted region is 4800cm^2 but must still be noted as it does leave room for untreated weeds.

5.5.2 Linear Accuracy Test

The results from the linear actuation also demonstrated a high level of accuracy. When mounting the linear movement housing to the rotational movement housing, the linear housing was strategically positioned close to its centre of gravity. This decision was made to minimize any unbalanced forces exerted on the main pivot point caused by the weight of the stepper motor. However, this design choice hindered the actuation arm from retracting to the centre of rotation. This created a circular dead zone around the main rotational pivot point of each arm; thus, the actuation arm could not target any points within a radius of 4.5cm from the central pivot point of the actuation arm.

This left an additional area of 127.23cm^2 unreachable by each set of actuation arms. Since the dead zone created by the reference key coincides with the area of this dead zone, it doesn't result in any additional untreated area left in the target region. With all four actuation arms operating, the combined dead zone area left untreated is 508.92cm^2 . This results in approximately 10.6% of the total targeted region being left untreated.

5.5.3 Combined Tests (single and multiple targets)

The combination of both the rotational and linear elements of the actuation arms provided favourable results in targeting weeds. In instances where the arm did not actuate exactly over the target, the splash radius of the liquid provided a degree of compensation for any deviations in accuracy, ensuring that the intended target was covered to an extent in all tests. In practical field conditions, when targeting weeds, the herbicide would be deposited with sufficient proximity to the weed such that a large portion of the dispensed herbicide would make contact with the weed.

The higher levels of inaccuracy were noted in the combined test compared to the individual tests of rotational and linear accuracy maybe since there was a slight inaccuracy in both the rotational and linear tests. The combination of these inaccuracies resulted in a total amplified inaccuracy, resulting in a greater overall deviation from the intended target. Improving both the rotational and linear accuracy would result in a higher level of accuracy achieved in the combination test.

When running multiple targets to the prototype it was noted that the targeting algorithm does not take into consideration the position of the pipes connected to the nozzles. In some instances, the pipes would obstruct the movement of the actuation arms, making them unable to reach a specific location. In addition to this, the position of the legs of the robot also presented some obstruction to the actuation arms.

5.6 Camera Vision

5.6.1 Object Detection

The Huskylens produced impressive results with regard to the distinction between crop and weed targets, even in scenarios where the arrangement of leaves was altered. However, it's worth noting that this function lacks, additional information about the detected object other than the object ID. This limitation affects the ability to precisely pinpoint the location of the crop or weed based solely through this function.

Additionally, the Huskylens encountered challenges in identifying a target when multiple objects were present within the frame, this is a highly likely scenario on the test ground. The camera also produced a constant false positive of Object ID1 even when there was no target present. These limitations make the data obtained from the Huskylens object detection function impractical for the intended scope of this project.

5.6.2 Colour Detection

The mounting height of the camera plays a crucial role in capturing an image of the entire target region. As outlined in the results section, the camera proves incapable of capturing the full target region in a single frame. In the user manual of the Huskylens, it was noted that the camera utilises the OV2640 image sensor, which is a relatively low-quality camera with a 2.0MP resolution. It's worth noting that if the camera could capture higher quality images, it might have the potential to identify colours within a broader range as the same colour identification algorithm could be applied over the higher quality images.

The results section illustrates that an increase in the mounting height of the camera negatively impacts the colour detection accuracy. However, with the camera mounted at a height of 45cm from the surface, the Huskylens was able to accurately detect targets within a field range of 58cm*40cm. This aligns perfectly with the width of the target region measuring 120cm*40cm.

The camera's colour recognition function provides an advantage in being able to extract precise coordinates of the targets. This information provides the precise positioning and dimensions of the identified targets, allowing for further analysis and application in the robotic system.

Due to time constraints, the full integration of the camera section was not included in the final design prototype, although all the required testing was completed regarding the chosen camera's capabilities along with the development of the camera movement system required to generate the required data. The software required for the camera system still needs to be implemented and tested concerning the accurate capture of the data.

5.7 Cart Design

The cart design fulfilled its intended purpose of securing all the necessary components in their designated positions. However, after the full assembly was completed, a few minor issues became apparent. The laser-cut legs were able to fully support the body of the robot, although it did exhibit a level of vulnerability due to the excess cutouts in specific areas. This resulted in some parts of the leg being more fragile and prone to breakage.

Furthermore, it was observed that the actuation arms were mounted in close proximity to the legs of the robot. This arrangement hindered the actuation arms, on either end of the robot from reaching certain locations. The back end of the actuation arm would collide with the legs of the robot, limiting its range of motion.

6. Conclusions

6.1 Nozzle Actuation

Based on the results obtained, it is evident that design one does not achieve the required level of precision in liquid deposition, with an exponential decrease in accuracy when targeting points further from the central pivot point. Nozzles should be mounted perpendicularly to the targeted surface to give the nozzle the best opportunity to perform with accuracy.

Design two introduces an excessive amount of weight on the extended actuation arm, potentially producing excess stress on the central actuation motor. Design three emerges as the optimal choice, due to the placement of heavy components at the main pivot point. Taking all factors into account, design three has been selected as the optimal choice to proceed with the prototyping process.

6.2 Arm Positioning

Upon careful analysis of the plots presented in Figures 30 and 31, it has been concluded that the optimal length for the actuation arms should be 25cm, as seen in Figures 31(c) and (d). This specific length ensures that the actuation arms are not too long such that the motor pivot point becomes unbalanced in the fully extended position introducing undue stress on the system.

It has been decided to position the arms at a distance of 30cm apart, as per the plotted data in Figure 31(d). This arrangement effectively eliminates dead points in the target range. This strategic placement optimizes the overall efficiency and coverage of the robotic system.

6.3 Nozzle Height and Design Test

The results section shows that the optimal mounting height for the nozzle is 15cm from the surface. This mounting height yielded the least splashing of the liquid deposits on the surface. Among the nozzle designs tested, the 1mm diameter keyway proved itself as the most efficient, significantly minimizing splashing in comparison to the other designed nozzle keyways while producing a small deposit of liquid.

This finding thus confirms that the 1mm diameter keyway nozzle should be used for the final prototype, mounted at a height of 15cm from above the target surface.

6.4 Herbicide Volume Test

To increase the precision achievable from the liquid dispensing system, the addition of a water pressure regulator could be added to the system. This would provide a more controlled and consistent pressure of liquid within the dispensing system. However, in applications where a high level of precision in dispensed liquid is not essential, the current liquid dispensing system could still be utilised.

There is an average variation of 0.233ml in this system's dispensing capabilities.

6.5 Nozzle Accuracy Test

6.5.1 Rotational Accuracy Test

While the dead zones identified cover a relatively small percentage of the overall targeted region, it is important to note that it does leave room for untreated weeds. For the current scope of this project, this dead zone is deemed acceptable. However, it should be given special attention in future iterations of the prototype. This will enhance the overall effectiveness of the system.

6.5.2 Linear Accuracy Test

As outlined in the discussion section, there was a notable dead zone introduced into the system as a result of the design of the actuation arm. To mitigate this issue, a staged targeting approach could be implemented. The robot would first focus on targeting all the weeds within its current reachable range. Thereafter, it would move forward, effectively repositioning the targets that were initially out of reach into a location now within the range of the actuation arms.

6.5.3 Combined Test (single and multiple targets)

The system was able to successfully target specific coordinates within an acceptable range, thanks to the compensation provided by the splash diameter of the deposited liquid. Additionally, when the system tried to target multiple points simultaneously, the control algorithm was able to determine a logical path of execution while still maintaining an acceptable level of accuracy. This achievement aligns with the primary goal of this project to target weeds, satisfying functional requirement RQ-02. Functional requirement RQ-01 is partially met as the system possesses the ability to cover a large portion of the target region, although there are some locations left untreated by this prototype.

6.6 Camera Vision

6.6.1 Object detection

Utilising the object detection feature on the Huskylens, the camera was unable to identify multiple targets present within one frame and provided no additional information with regard to the precise location of the targets within the frame. These limitations render the data obtained from the Huskylens impractical for the intended scope of this project.

6.6.2 Colour detection

The colour detection feature of the Huskylens has proven its superiority for this project. It enables the extraction of specific target locations and the identification of multiple targets within a single frame in line with functional requirement RQ-03. Based on the findings in the results section and discussion, the Huskylens should be mounted at a height of 45cm from the surface. This positioning provides a field range large enough it to identify targets across the entire width of the target region in one frame.

To capture the entire target region, a stepped scanning motion should be employed. This technique will involve capturing multiple images of the target region and stitching together each frame to generate the entire target map.

6.7 Cart Design

To improve the overall efficiency of this robot and ensure the design is durable, there are a few modifications should be implemented in the design. The legs should feature fewer cutouts as they were simply included for aesthetic purposes and offer no additional features to the design. In addition to this, the pivot points of the actuation arms should be mounted further away from the legs such that there are no obstacles in the way of the actuation arms.

Based on the conclusions drawn from each section above, it is evident that the final prototype successfully operated within an acceptable range according to the objectives outlined in this study. Specifically, it met the acceptance criteria for functional requirement RQ-02 by accurately dispensing liquid at the intended target location. However, functional requirements RQ-01 and RQ-03 were only partially fulfilled. While the prototype effectively covered a substantial portion of the target region, some areas remained untreated, indicating partial satisfaction of RQ-01. Due to time constraints, testing the system's ability to meet the functional requirement RQ-03 was not feasible. However, the camera system demonstrated its capability to differentiate between distinct colours, having been tested and trained with relevant data. The full integration of the coding aspect of the Huskylens should result in fully satisfying functional requirement RQ-03.

7. Recommendations

If this project were to be further developed, the initial focus should be on the integration of the camera system into the overall design of the robot. Additionally, there are areas in the existing prototype that could benefit from further refinement.

7.1 Dead Zone Mitigation

It has been observed that due to the design of the actuation arm housing unit, a large portion of the target range was left unreachable. A straightforward fix for this issue would be through a revision of the design of the actuation arm housing. It was noted that the rack failed to achieve complete retraction to the central pivot point, resulting in this dead zone. In the proposed revision of the actuation arm housing must accommodate the full retraction of the rack such that targets around the central pivot point can be targeted as intended.

7.2 Revision of the Coding Structure

The target allocation algorithm utilised in this prototype employs a simplified approach to the allocation process, categorizing each target exclusively reachable by a specific set of arms. However, the design of the project enables certain sections of the target region reachable by more than one set of arms in some scenarios. Thus, select targets may be designated for allocation to either of the two arms. A revised sorting algorithm should be implemented to determine the most efficient strategy for targeting these points.

Furthermore, the sorting of targets allocated to the individual arms in ascending order of the rotational actuation may not be the most optimal approach for targeting these points. A more efficient means to determine the path of execution should be developed. One strategy could be through the comparison of the absolute distance between all targets allocated to the arm and target these points based on the shortest distance to each target.

7.3 Addition of Pressure Regulator

From the conclusions drawn, the incorporation of a water pressure regulator into the liquid dispensing system would increase the precision achievable with this robot, enabling the robot's usage for more precise applications. Further testing would be required to confirm the effectiveness of the pressure regulator.

7.4 Revision of Leg Design

As noted in the discussion and conclusion, the current design of the legs renders them susceptible to damage due to the design and positioning of cutouts on the design. Future iterations should improve on this design with the intention of increasing the strength and durability of the prototype. Additionally, it was observed that the current positioning of the legs limited the range of motion of the actuation arms. To address this the legs should be mounted out of the arms range in future iterations of the project.

8. List of References

- [1] A. T. Meshram, A. V. Vanalkar, K. B. Kalambe, and A. M. Badar, "Pesticide spraying robot for precision agriculture: A categorical literature review and future trends," *Journal of Field Robotics*, vol. 39, no. 2, pp. 153-171, 2022, doi: 10.1002/rob.22043.
- [2] T. Utstumo *et al.*, "Robotic in-row weed control in vegetables," *Computers and Electronics in Agriculture*, vol. 154, pp. 36-45, 11/01 2018, doi: 10.1016/j.compag.2018.08.043.
- [3] F. Urdal, T. Utstumo, J. K. Vatne, S. A. A. Ellingsen, and J. T. Gravdahl, "Design and control of precision drop-on-demand herbicide application in agricultural robotics," 2014: IEEE, doi: 10.1109/icarcv.2014.7064570. [Online]. Available: <https://dx.doi.org/10.1109/icarcv.2014.7064570>
- [4] D. E. Martin, W. E. Woldt, and M. A. Latheef, "Effect of Application Height and Ground Speed on Spray Pattern and Droplet Spectra from Remotely Piloted Aerial Application Systems," *Drones*, vol. 3, no. 4, p. 83, 2019, doi: 10.3390/drones3040083.
- [5] C. D. Bellicoso *et al.*, "Advances in real-world applications for legged robots," *Journal of Field Robotics*, vol. 35, no. 8, pp. 1311-1326, 2018, doi: 10.1002/rob.21839.
- [6] D. C. Slaughter, D. K. Giles, and D. Downey, "Autonomous robotic weed control systems: A review," *Computers and Electronics in Agriculture*, vol. 61, no. 1, pp. 63-78, 2008/04/01/ 2008, doi: <https://doi.org/10.1016/j.compag.2007.05.008>.
- [7] R. Raja, D. C. Slaughter, S. A. Fennimore, and M. C. Siemens, "Real-time control of high-resolution micro-jet sprayer integrated with machine vision for precision weed control," *Biosystems Engineering*, vol. 228, pp. 31-48, 2023/04/01/ 2023, doi: <https://doi.org/10.1016/j.biosystemseng.2023.02.006>.
- [8] S. Kiani and A. Jafari, "Crop detection and positioning in the field using discriminant analysis and neural networks based on shape features," *Journal of Agricultural Science and Technology*, vol. 14, pp. 755-765, 07/01 2012.
- [9] P. Lottes, J. Behley, N. Chebrolu, A. Milioto, and C. Stachniss, "Joint Stem Detection and Crop-Weed Classification for Plant-specific Treatment in Precision Farming," *arXiv pre-print server*, 2018-06-09 2018, doi: None
arxiv:1806.03413.
- [10] L. Elstone, K. Y. How, S. Brodie, M. Z. Ghazali, W. P. Heath, and B. Grieve, "High speed crop and weed identification in lettuce fields for precision weeding," *Sensors*, vol. 20, no. 2, p. 455, 2020.
- [11] H. S. Midtiby, T. M. Giselsson, and R. N. Jørgensen, "Estimating the plant stem emerging points (PSEPs) of sugar beets at early growth stages," *Biosystems Engineering*, vol. 111, no. 1, pp. 83-90, 2012, doi: 10.1016/j.biosystemseng.2011.10.011.
- [12] P. K. Jensen, "Target precision and biological efficacy of two nozzles used for precision weed control," *Precision Agriculture*, vol. 16, no. 6, pp. 705-717, 2015, doi: 10.1007/s11119-015-9399-4.
- [13] D. C. Vadillo, T. R. Tuladhar, A. C. Mulji, S. Jung, S. D. Hoath, and M. R. Mackley, "Evaluation of the inkjet fluid's performance using the "Cambridge Trimaster" filament stretch and break-up device," *Journal of Rheology*, vol. 54, pp. 261-282, 2010.
- [14] H. Dong, W. W. Carr, and J. F. Morris, "An experimental study of drop-on-demand drop formation," *Physics of Fluids*, vol. 18, p. 072102, 2006.
- [15] S. D. Hoath, S. Jung, and I. M. Hutchings, "A simple criterion for filament break-up in drop-on-demand inkjet printing," *Physics of Fluids*, vol. 25, no. 2, 2013, doi: 10.1063/1.4790193.

- [16] M. Gonzalez-de-Soto, L. Emmi, M. Perez-Ruiz, J. Aguera, and P. Gonzalez-de-Santos, "Autonomous systems for precise spraying–Evaluation of a robotised patch sprayer," *Biosystems engineering*, vol. 146, pp. 165-182, 2016.
- [17] D. Downey, D. K. Giles, and D. Slaughter, "Pulsed-jet microspray applications for high spatial resolution of deposition on biological targets," *Atomization and Sprays*, vol. 14, no. 2, 2004.

9. Appendix A

GitHub link to code utilised in the control of the robotic system:

https://github.com/KayuranN/EEE4022S_PrecisionHerbicideSprayer/tree/main/Arduino%20Code%20Files

GitHub link to all the modelled parts utilised in this project:

https://github.com/KayuranN/EEE4022S_PrecisionHerbicideSprayer/tree/main/Modeled%20Components

10. Appendix B

Component	Quantity	Unit Price	Total Price
Solenoid Valves	4	R101	R404,00
Stepper motor and Driver	8	R39	R312,00
Water Pump	1	R102	R102,00
Huskylens	1	Own Components	Own Components
Arduino Mega	1	Own Components	Own Components
8mm PVC tube	1	R105	R105,00
Veroboard	1	R44	R44,00
Jumper cables (40)	2	R23	R46,00
N20 motor	1	R101	R101,00
6V Dc motor	2	Own Components	Own Components
Magnetic encoder	1	R89	R89,00
Optical Encoder	2	Own Components	Own Components
TIP122 transistors	5	Own Components	Own Components
4004 Diode	5	Own Components	Own Components
Pin connectors	3	Own Components	Own Components
TOTAL			R1203

11. EBE Faculty: Assessment of Ethics in Research Projects

Any person planning to undertake research in the Faculty of Engineering and the Built Environment at the University of Cape Town is required to complete this form before collecting or analysing data. When completed it should be submitted to the supervisor (where applicable) and from there to the Head of Department. If any of the questions below have been answered YES, and the applicant is NOT a fourth year student, the Head should forward this form for approval by the Faculty EIR committee: submit to Ms Zulpha Geyer (Zulpha.Geyer@uct.ac.za; Chem Eng Building, Ph 021 650 4791). Students must include a copy of the completed form with the final year project when it is submitted for examination.

Name of Principal

Researcher/Student: Kayuran Naicker

Department: ELECTRICAL ENGINEERING

If a Student: YES **Degree:** BSc. Eng
Mechatronics

Supervisor: Boitumelo Dikoko

If a Research Contract indicate source of funding/sponsorship:

N/A

Research Project

Title: Precision Herbicide Sprayer for an Agricultural Robot

Overview of ethics issues in your research project:

Question 1: Is there a possibility that your research could cause harm to a third party (i.e. a person not involved in your project)?	YES	NO
Question 2: Is your research making use of human subjects as sources of data? If your answer is YES, please complete Addendum 2.	YES	NO
Question 3: Does your research involve the participation of or provision of services to communities? If your answer is YES, please complete Addendum 3.	YES	NO
Question 4: If your research is sponsored, is there any potential for conflicts of interest? If your answer is YES, please complete Addendum 4.	YES	NO

If you have answered YES to any of the above questions, please append a copy of your research proposal, as well as any interview schedules or questionnaires (Addendum 1) and please complete further addenda as appropriate.

I hereby undertake to carry out my research in such a way that

- there is no apparent legal objection to the nature or the method of research; and
- the research will not compromise staff or students or the other responsibilities of the University;
- the stated objective will be achieved, and the findings will have a high degree of validity;
- limitations and alternative interpretations will be considered;
- the findings could be subject to peer review and publicly available; and
- I will comply with the conventions of copyright and avoid any practice that would constitute plagiarism.

Signed by:

	Full name and signature	Date
Principal Researcher/Student:	Kayuran Naicker	30 October 2023

This application is approved by:

Supervisor (if applicable):	Boitumelo Dikoko	30 October 2023
HOD (or delegated nominee): Final authority for all assessments with NO to all questions and for all undergraduate research.	Janine Buxey	30 October 2023
Chair : Faculty EIR Committee For applicants other than undergraduate students who have answered YES to any of the above		